

Fast Projected Newton-like Method for Precision Matrix Estimation with Nonnegative Partial Correlations

Jiaxi Ying ^{*} José Vinícius de M. Cardoso [†] Jian-Feng Cai [‡] Daniel P. Palomar [§]

December 6, 2021

Abstract

We study the problem of estimating precision matrices in multivariate Gaussian distributions where all partial correlations are nonnegative, also known as multivariate totally positive of order two (MTP₂). Such models have received significant attention in recent years, primarily due to interesting properties, *e.g.*, the maximum likelihood estimator exists with as few as two observations regardless of the underlying dimension. We formulate this problem as a weighted ℓ_1 -norm regularized Gaussian maximum likelihood estimation under MTP₂ constraints. On this direction, we propose a novel projected Newton-like algorithm that incorporates a well-designed approximate Newton direction, which results in our algorithm having the same orders of computation and memory costs as those of first-order methods. We prove that the proposed projected Newton-like algorithm converges to the minimizer of the problem. We further show, both theoretically and experimentally, that the minimizer of our formulation using the weighted ℓ_1 -norm is able to recover the support of the underlying precision matrix correctly without requiring the *incoherence* condition present in ℓ_1 -norm based methods. Experiments involving synthetic and real-world data demonstrate that our proposed algorithm is significantly more efficient, from a computational time perspective, than the state-of-the-art methods. Finally, we apply our method in financial time-series data, which are well-known for displaying positive dependencies, where we observe a significant performance in terms of *modularity* value on the learned financial networks.

Keywords: Two-metric projection method, Graph signal processing, M-matrix, MTP₂ distributions, Support recovery consistency, Projected Newton-like algorithm.

1 Introduction

We consider the problem of estimating precision matrices (*i.e.*, inverse covariance matrices) in multivariate Gaussian distributions where all partial correlations are nonnegative. Such models arise in a variety of applications such as actuarial sciences (Denuit et al., 2006), taxonomic reasoning (Slawski and Hein, 2015), financial markets (Agrawal et al., 2020), factor analysis in psychometrics (Lauritzen et al., 2019), and graph signal processing (Egilmez et al., 2017; Dong et al., 2019). For example, instruments in equity markets are often positively dependent as a result of the market factor (Agrawal et al., 2020; Cardoso et al., 2020).

^{*}Department of Electronic and Computer Engineering, The Hong Kong University of Science and Technology, Clear Water Bay, Hong Kong SAR; Email: jx.ying@connect.ust.hk.

[†]Department of Electronic and Computer Engineering, The Hong Kong University of Science and Technology, Clear Water Bay, Hong Kong SAR; Email: jvdmc@connect.ust.hk.

[‡]Department of Mathematics, The Hong Kong University of Science and Technology, Clear Water Bay, Hong Kong SAR; Email: jfcai@ust.hk.

[§]Department of Electronic and Computer Engineering, Department of Industrial Engineering and Data Analytics, The Hong Kong University of Science and Technology, Clear Water Bay, Hong Kong SAR; Email: palomar@ust.hk.

Estimating precision matrices is closely related to learning Gaussian graphical models, where the zero pattern of the precision matrix is associated with the graph structure of a Gaussian Markov random field that encodes the conditional independence between random variables. The problem of estimating precision matrices has been extensively studied in the literature. One well-known method is graphical lasso (Banerjee et al., 2008; d’Aspremont et al., 2008; Yuan and Lin, 2007), which is formulated as an ℓ_1 -norm regularized Gaussian maximum likelihood estimation. Various extensions of graphical lasso and their theoretical properties have also been studied (Ravikumar et al., 2011; Mazumder and Hastie, 2012; Shojaie and Michailidis, 2010; Hsieh et al., 2012, 2013; Yang et al., 2012, 2015; Honorio et al., 2012; McCarter and Kim, 2016; Chen et al., 2018). In this paper, we focus on estimating the precision matrix with nonnegative partial correlations, *i.e.*, all the off-diagonal elements of the precision matrix are nonpositive. The resulting precision matrix is a symmetric *M-matrix*. Such property is also known as multivariate totally positive of order two (MTP₂) (Fallat et al., 2017; Lauritzen et al., 2019). For ease of presentation, we call the nonpositivity constraints on the off-diagonal elements of precision matrices as MTP₂ constraints.

Estimating precision matrices under MTP₂ constraints has become an active research topic (Slawski and Hein, 2015; Fallat et al., 2017; Lauritzen et al., 2019, 2021; Wang et al., 2020; Pavez and Ortega, 2016; Egilmez et al., 2017; Pavez et al., 2018; Soloff et al., 2020; Kelner et al., 2020). One interesting result provided in Slawski and Hein (2015); Lauritzen et al. (2019) shows that the maximum likelihood estimator for MTP₂ Gaussian distributions exists with as few as two observations regardless of the underlying dimension, which leads to a drastic reduction from $n \geq p$ in the Gaussian case without MTP₂ constraints, where n and p denote the sample size and problem dimension, respectively. Aside from Gaussian distributions, the advantages of MTP₂ constraints were also explored in the binary exponential family, where it was proved that the maximum likelihood estimator may exist with only $n = p$ observations (Lauritzen et al., 2021), while $n \geq 2^p$ is required in case MTP₂ constraints are not included. Such advantages of MTP₂ constraints (Slawski and Hein, 2015; Lauritzen et al., 2019, 2021) have been critical in high-dimensional regimes, where the number of samples is usually limited compared to the problem dimension. In recent years, there is growing interest in estimating precision matrices under MTP₂ constraints in graph signal processing (Pavez and Ortega, 2016; Egilmez et al., 2017; Pavez et al., 2018). A precision matrix satisfying MTP₂ constraints can be viewed as a generalized graph Laplacian, which enjoys the spectral property that its eigenvalues and eigenvectors can be interpreted as spectral frequencies and Fourier bases, thus it can be used in computing the graph Fourier transform (Shuman et al., 2013; Ortega et al., 2018). The MTP₂ property was also studied in portfolio allocation (Agrawal et al., 2020) and structure recovery (Wang et al., 2020; Kelner et al., 2020).

The problem of precision matrix estimation with nonnegative partial correlations can be formulated as the Gaussian maximum likelihood estimation under MTP₂ constraints, which is a sign-constrained log-determinant program. Recent works (Slawski and Hein, 2015; Pavez and Ortega, 2016; Egilmez et al., 2017) proposed algorithms based on block coordinate descent (BCD). Such algorithms cyclically update each column/row of the primal or dual variable by solving a nonnegative quadratic program. BCD-type algorithms (Slawski and Hein, 2015; Pavez and Ortega, 2016; Egilmez et al., 2017) can be efficient for low-dimensional problems, while they become time-consuming in high-dimensional cases, because of the need to solve a large number of nonnegative quadratic programs. Apart from BCD-type algorithms, this sign-constrained log-determinant program can also be solved by the projected gradient method, which is usually computationally efficient. However, they often suffer from low convergence rate for large-scale optimization problems because of bad condition numbers (Bertsekas, 2016). Therefore, it remains to develop efficient and scalable algorithms to solve the Gaussian maximum likelihood estimation under MTP₂ constraints.

In this paper, we propose a fast projected Newton-like algorithm for estimating precision matrices under MTP₂ constraints. It is well-known that second-order algorithms usually require fewer iterations than first-order methods, while they often show issues related to expensive costs in computation and memory. Note that a straightforward implementation of the second-order method to solve our problem would be too expensive in terms of computation and memory costs because it involves calculating and storing the inverse of the (approximate) Hessian matrix, which has dimension $p^2 \times p^2$, or solving a system of linear equations of

the same dimension. The main contributions of this paper are threefold:

- We propose a fast projected Newton-like method for precision matrix estimation under MTP_2 constraints. More specifically, we propose a variable partitioning scheme which separates variables into two groups, *restricted* and *free*, at each iteration. The *restricted* are directly set as zero, and the *free* are updated in a well-designed approximate Newton direction. The proposed algorithm requires the same orders of computation and memory costs as those of projected gradient method. We prove that our algorithm converges to the minimizer of the problem of interest, and the set of *free* variables identifies the support of the minimizer in a finite number of iterations.
- It is known that the *incoherence* condition on the underlying precision matrix is typically required for graphical lasso to be selection consistent. However, such condition is usually restrictive in practice and is not straightforward to interpret. To remove this restriction, we adopt the weighted ℓ_1 -norm in our formulation, where the regularization weights are computed adaptively based on an initial estimator. We show, both theoretically and experimentally, that the minimizer of our formulation achieves support recovery consistency without requiring the *incoherence* condition.
- Numerical experiments on both synthetic and real-world data sets provide strong evidence that our algorithm costs significantly less time to converge to the minimizer than state-of-the-art methods. Numerical results also demonstrate that the sample size required for successful support recovery has approximate logarithmic dependence on the problem dimension. Finally, we apply our method in financial time-series data, which are well-known for displaying positive dependencies, where we observe a significant performance in terms of *modularity* value on the learned financial networks.

The remainder of this paper is organized as follows. Problem formulation and related work are provided in Section 2. We propose a novel projected Newton-like algorithm in Section 3, and present theoretical results on convergence analysis and support recovery consistency in Section 4. Experimental results are provided in Section 5, and conclusions are made in Section 6. The proofs are provided in Appendix A. The source code of the algorithm proposed in this paper is publicly available at <https://github.com/jxying/mtp2>.

Notation: Lower case bold letters denote vectors and upper case bold letters denote matrices. Both X_{ij} and $[\mathbf{X}]_{ij}$ denote the (i, j) -th entry of \mathbf{X} . $[p]$ denotes the set $\{1, \dots, p\}$, and $[p]^2$ denotes the set $\{1, \dots, p\} \times \{1, \dots, p\}$. Let \otimes be the Kronecker product and \odot be the entry-wise product, and $\text{supp}(\mathbf{X}) = \{(i, j) \in [p]^2 \mid X_{ij} \neq 0\}$. $\text{vec}(\mathbf{X})$ denotes the vectorized version of \mathbf{X} . \mathbf{X}^\top denotes transpose of \mathbf{X} . $\|\mathbf{x}\|$, $\|\mathbf{X}\|_{\text{F}}$ and $\|\mathbf{X}\|_2$ denote Euclidean norm, Frobenius norm and operator norm, respectively. $\|\mathbf{X}\|_{\infty}$ denotes the $\ell_{\infty}/\ell_{\infty}$ -operator norm given by $\|\mathbf{X}\|_{\infty} := \max_{i=1, \dots, p} \sum_{j=1}^p |X_{ij}|$. Let $\|\mathbf{X}\|_{\max} = \max_{i,j} |X_{ij}|$ and $\|\mathbf{X}\|_{\min} = \min_{i,j} |X_{ij}|$. \mathbb{S}_+^p and \mathbb{S}_{++}^p denote the sets of positive semi-definite and positive definite matrices with the dimension $p \times p$, respectively. For functions $f(n)$ and $g(n)$, we use $f(n) \gtrsim g(n)$ if $f(n) \geq cg(n)$, for some constant $c \in (0, +\infty)$. If \mathcal{S} and \mathcal{S}' are two sets of indexes $(i, j) \in [p]^2$, $\mathbf{A} \in \mathbb{R}^{p \times p}$, and $\mathbf{B} \in \mathbb{R}^{p^2 \times p^2}$, then $[\mathbf{A}]_{\mathcal{S}}$ denotes the vector with the dimension $|\mathcal{S}|$ which contains the elements of \mathbf{A} indexed by \mathcal{S} , and $[\mathbf{B}]_{\mathcal{S}\mathcal{S}'}$ denotes the $|\mathcal{S}| \times |\mathcal{S}'|$ matrix with rows and columns of \mathbf{B} indexed by \mathcal{S} and \mathcal{S}' , respectively.

2 Problem Formulation and Related Work

In this section, we first introduce the problem formulation, then present related works.

2.1 Problem Formulation

Let $\mathbf{y} = (y_1, \dots, y_p)$ be a zero-mean p -dimensional random vector following $\mathbf{y} \sim \mathcal{N}(\mathbf{0}, \mathbf{\Sigma})$, where $\mathbf{\Sigma}$ is the covariance matrix. We consider the problem of estimating the precision matrix $\mathbf{\Theta} := \mathbf{\Sigma}^{-1}$ given n independent and identically distributed observations $\{\mathbf{y}^{(k)}\}_{k=1}^n$.

This problem is motivated in Gaussian graphical models. More specifically, we denote an undirected graph by $\mathcal{G} = (V, E)$, where $V = \{1, \dots, p\}$ is the vertex set and E is the edge set. We associate the random variables y_1, \dots, y_p with the vertex set V . Then, the random vector $\mathbf{y} = (y_1, \dots, y_p)$ forms a Gaussian Markov random field with respect to a graph $\mathcal{G} = (V, E)$, where

$$\begin{aligned}\Theta_{ij} \neq 0 &\iff (i, j) \in E \ \forall i \neq j, \\ \Theta_{ij} = 0 &\iff y_i \perp\!\!\!\perp y_j \mid \mathbf{y}_{[p] \setminus \{i, j\}}.\end{aligned}$$

In this paper, we focus on multivariate Gaussian distributions that satisfy the MTP_2 property, a strong form of pairwise positive dependence. A multivariate real-valued distribution with density function f , with respect to a product measure, is MTP_2 if

$$f(\mathbf{x})f(\mathbf{y}) \leq f(\mathbf{x} \wedge \mathbf{y})f(\mathbf{x} \vee \mathbf{y}),$$

where \wedge and \vee denote the coordinate-wise minimum and maximum, respectively. In particular, a multivariate Gaussian distribution with a positive definite precision matrix Θ is MTP_2 if and only if Θ is a symmetric M -matrix (Bølviken, 1982; Karlin and Rinott, 1983), *i.e.*, $\Theta_{ij} \leq 0$ for any $i \neq j$, which equivalently says that all partial correlations are nonnegative. Note that the partial correlation between any two variables y_i and y_j conditioned on all the others is equal to $-\Theta_{ij}/\sqrt{\Theta_{ii}\Theta_{jj}}$. MTP_2 Gaussian graphical models are also known as *attractive* Gaussian graphical models (Malioutov et al., 2006; Anandkumar et al., 2012).

The focus of this paper is the problem of estimating the precision matrix in a MTP_2 Gaussian distribution given independent and identically distributed observations $\mathbf{y}^{(1)}, \dots, \mathbf{y}^{(n)} \in \mathbb{R}^p$. Let $\mathbf{S} = \frac{1}{n} \sum_{i=1}^n \mathbf{y}^{(i)} (\mathbf{y}^{(i)})^\top$ be the sample covariance matrix. We consider estimating the precision matrix Θ by solving the following weighted ℓ_1 -norm regularized Gaussian maximum likelihood estimation under MTP_2 constraints:

$$\begin{aligned}\mathbf{X}^* := \arg \min_{\mathbf{X} \in \mathcal{M}^p} & \quad -\log \det(\mathbf{X}) + \text{tr}(\mathbf{X}\mathbf{S}) + \sum_{i \neq j} \lambda_{ij} |X_{ij}|, \\ \text{subject to} & \quad X_{ij} = 0, \ \forall (i, j) \in \mathcal{E},\end{aligned}\tag{1}$$

where λ_{ij} is the regularization parameter, \mathcal{E} is the disconnectivity set defined as the pairs of nodes that are forced to be disconnected, and \mathcal{M}^p is the set of all p -dimensional, symmetric, non-singular M -matrices, which is defined by

$$\mathcal{M}^p := \{\mathbf{X} \in \mathbb{S}_{++}^p \mid X_{ij} \leq 0, \ \forall i \neq j\}.\tag{2}$$

Imposing the disconnectivity set \mathcal{E} in (1) can guarantee that the corresponding pairs of nodes will be disconnected in the learned graph. We note that the disconnectivity set can be obtained in several ways: (i) it is often the case that some edges between nodes must not exist according to prior knowledge; (ii) it can be estimated from initial estimators; (iii) it can be obtained in some tasks of learning structural graphs such as bipartite where the partition of the nodes is given.

One interesting result reported in Pavez et al. (2018) shows that the entry $[\mathbf{X}^*]_{ij}$ of the minimizer of Problem (1) must be zero if $S_{ij} \leq \lambda_{ij}$, implying that part of zero patterns can be predicted in advance. Moreover, we will show in Section 4 that the weighted ℓ_1 regularization does not require the *incoherence* condition to recover the support correctly, while it is almost necessary for the ℓ_1 regularization.

2.2 Related Work

Estimating precision matrices under Gaussian graphical models has received broad interest in statistical machine learning and optimization. One well-known method is graphical lasso (Banerjee et al., 2008; d’Aspremont et al., 2008; Yuan and Lin, 2007; Ravikumar et al., 2011), which minimizes the ℓ_1 -regularized Gaussian negative log-likelihood. One of the major difficulties in solving this optimization problem is on the nonsmoothness of the objective function, because of the ℓ_1 -norm regularization. To handle this nuisance, a number of works solved the problem from the dual perspective, which is smooth, using different algorithms

such as block coordinate descent (Banerjee et al., 2008; Friedman et al., 2008), gradient projection (Duchi et al., 2008), accelerated gradient descent (Lu, 2009), and projected quasi-Newton (Schmidt et al., 2009). In another direction, some works proposed algorithms to directly solve the primal problem such as Nesterov’s gradient with smoothed ℓ_1 -norm (d’Aspremont et al., 2008), greedy coordinate descent (Scheinberg and Rish, 2010), alternating linearization (Scheinberg et al., 2010), proximal-Newton (Dinh et al., 2013), primal proximal-point with Newton-CG (Wang et al., 2010), inexact primal-dual interior-point (Li and Toh, 2010), and Newton’s method with quadratic approximation (Hsieh et al., 2011; Oztoprak et al., 2012; Hsieh et al., 2014). We note that the graphical lasso formulation under Gaussian graphical models is an unconstrained nonsmooth optimization problem, while our problem in (1) is smooth and constrained. Therefore, the difficulties in solving the two problems are inherently different, and the algorithms mentioned above cannot be directly extended to solve our problem. It is worth mentioning that, among the aforementioned algorithms, the ones proposed in Schmidt et al. (2009); Dinh et al. (2013); Wang et al. (2010); Li and Toh (2010); Hsieh et al. (2011); Oztoprak et al. (2012); Hsieh et al. (2014) are second-order algorithms, where iterative methods are required to obtain the (approximate) Newton direction such as preconditioned conjugate gradient, fixed-point iteration, and coordinate descent, while our proposed algorithm computes the search direction more efficiently as shown in Section 3.

To estimate precision matrices under MTP_2 constraints, several algorithms based on the BCD scheme were proposed in Slawski and Hein (2015); Pavez and Ortega (2016); Egilmez et al. (2017). Slawski and Hein (2015) updates a single column/row of the primal variable at a time by solving a nonnegative quadratic program through the block principle pivoting algorithm, while the remaining variable are kept fixed. All the columns/rows are updated in a cycle, and the updating is repeated until convergence. Pavez and Ortega (2016) followed the similar strategy, but solved the dual problem. Their algorithm avoids storing a dense covariance matrix, and thus can be more memory efficient. Both works Slawski and Hein (2015); Pavez and Ortega (2016) aimed to solve Problem (1) without the disconnectivity constraint. More recently, Egilmez et al. (2017) proposed a BCD algorithm that enables the disconnectivity constraint, and it can be extended to estimate a precision matrix that is a diagonally dominant M -matrix. Regarding computational complexity, BCD-type algorithms (Slawski and Hein, 2015; Pavez and Ortega, 2016; Egilmez et al., 2017) need to solve p nonnegative quadratic programs per cycle, and thus requires $O(p^4)$ operations in each cycle, which is computationally prohibitive in high-dimensional problems.

The MTP_2 constraints lead Problem (1) to be a smooth constrained optimization problem. While this problem can be tackled by simple projected gradient method whose computation and memory costs are modest at each iteration, it often requires a very large number of iterations for convergence in high-dimensional problems. To reduce the iteration complexity, one may consider the projected Newton method (Bertsekas, 1982), which was originally designed for box-constrained optimization problems and proved to have an asymptotic superlinear rate of convergence. However, such algorithm is not suitable to solve our problem, because it needs to store a huge Hessian matrix which requires $O(p^4)$ memory and evaluate the inverse of some principle submatrix of the Hessian which requires $O(p^6)$ operations. To reduce the computation and memory costs, Kim et al. (2010) extended the limited-memory Boyden-Fletcher-Goldfarb-Shanno (L-BFGS) (Nocedal, 1980) which uses curvature information from only the most recent iterations to construct the Hessian approximation, and proposed the projected quasi-Newton method with L-BFGS, of which the subsequence convergence was established. Such algorithm only requires $O((m + p)p^2)$ operations and $O(mp^2)$ memory in each iteration, where m is the number of iterations stored for approximating the inverse Hessian. Note that the aforementioned methods (Bertsekas, 1982; Kim et al., 2010) are in the framework of the two-metric projection method (Gafni and Bertsekas, 1984), which embodies two different metrics used to determine the search direction and the projection. In this paper, our proposed fast projected Newton-like method is also based on the two-metric projection framework. We design an approximate Newton direction that can be computed efficiently and implemented easily. Consequently, the proposed algorithm requires the same orders of computation and memory costs as those of the projected gradient method, while the former enjoys the benefits of the second-order information, leading to a faster convergence than the latter. The two-metric

projection framework has been explored in many other problems such as nonnegative image reconstruction (Bardsley and Vogel, 2004; Landi and Piccolomini, 2013), nonnegative matrix approximation (Kim et al., 2007), total variation (Jiménez and Sra, 2011), image deblurring (Landi and Piccolomini, 2012), group fused lasso (Wytock et al., 2014), phase recovery (Herring et al., 2019), and inverse heat convection (Rothermel and Schuster, 2021), and its iteration complexity has been studied in Xie and Wright (2021).

3 Proposed Algorithm

In this section, we propose a fast projected Newton-like (FPN) algorithm to solve the weighted ℓ_1 -norm regularized Gaussian maximum likelihood estimation under MTP₂ constraints as shown in (1).

We note that Problem (1) is a constrained convex optimization problem. The constraints in (1) can be rewritten as $\mathbf{X} \in \Omega \cap \mathbb{S}_{++}^p$, where Ω is defined as

$$\Omega := \{ \mathbf{X} \in \mathbb{R}^{p \times p} \mid X_{ij} = 0, \forall (i, j) \in \mathcal{E}; X_{ij} \leq 0, \forall i \neq j \}.$$

It is observed that the set Ω is convex and closed, and we can handle this constraint by a projection \mathcal{P}_Ω onto Ω with respect to the Frobenius norm defined by

$$[\mathcal{P}_\Omega(\mathbf{A})]_{ij} = \begin{cases} 0 & \text{if } (i, j) \in \mathcal{E}, \\ A_{ij} & \text{if } i = j, \\ \min(A_{ij}, 0) & \text{if } (i, j) \notin \mathcal{E} \text{ and } i \neq j. \end{cases} \quad (3)$$

But the positive definite constraint set \mathbb{S}_{++}^p is not closed, and thus cannot be handled by a projection. We impose the positive definiteness by a backtracking line search method (more details can be found in Section 3.3).

To solve Problem (1), we start with the projected gradient method, which can be formulated as

$$\mathbf{X}_{k+1} = \mathcal{P}_\Omega(\mathbf{X}_k - \gamma_k \nabla f(\mathbf{X}_k)), \quad (4)$$

where γ_k is the step size in the k -th iteration, f is the objective function of Problem (1), and $\nabla f(\mathbf{X}_k)$ denotes the gradient at \mathbf{X}_k . The projected gradient descent can be viewed as an instance of the successive convex approximation approach (Scutari et al., 2014), which solves a sequence of convex approximation problems. More specifically, the iterate \mathbf{X}_{k+1} in (4) is the closed-form solution of the following problem:

$$\underset{\mathbf{X} \in \Omega}{\text{minimize}} f(\mathbf{X}_k) + \langle \nabla f(\mathbf{X}_k), \mathbf{X} - \mathbf{X}_k \rangle + \frac{1}{2\gamma_k} \|\mathbf{X} - \mathbf{X}_k\|_F^2, \quad (5)$$

where the objective function in (5) is a quadratic approximation of f around the point \mathbf{X}_k . The projected gradient method is a first-order iterative method, which uses the negative gradient as the descent direction. To accelerate the convergence, one may construct a better quadratic approximation and solve the following problem:

$$\underset{\mathbf{X} \in \Omega}{\text{minimize}} f(\mathbf{X}_k) + \langle \nabla f(\mathbf{X}_k), \mathbf{X} - \mathbf{X}_k \rangle + \frac{1}{2\gamma_k} \text{vec}(\mathbf{X} - \mathbf{X}_k)^\top \mathbf{M}_k \text{vec}(\mathbf{X} - \mathbf{X}_k), \quad (6)$$

where $\mathbf{M}_k \in \mathbb{R}^{p^2 \times p^2}$ is a positive definite symmetric matrix, which is an approximation of the Hessian at \mathbf{X}_k , and $\text{vec}(\mathbf{X}) \in \mathbb{R}^{p^2}$ denotes the vectorized version of $\mathbf{X} \in \mathbb{R}^{p \times p}$. Define a matrix $\mathbf{P}_k \in \mathbb{R}^{p \times p}$ by

$$\text{vec}(\mathbf{P}_k) = \mathbf{M}_k^{-1} \text{vec}(\nabla f(\mathbf{X}_k)). \quad (7)$$

Then Problem (6) can be equivalently expressed as

$$\underset{\mathbf{X} \in \Omega}{\text{minimize}} \|\mathbf{X} - \mathbf{X}_k + \gamma_k \mathbf{P}_k\|_{\mathbf{M}_k}^2, \quad (8)$$

where $\|\cdot\|_{\mathbf{M}_k}$ is a quadratic norm defined by $\|\mathbf{A}\|_{\mathbf{M}_k} = \langle \text{vec}(\mathbf{A}), \mathbf{M}_k \text{vec}(\mathbf{A}) \rangle^{\frac{1}{2}}$ for any $\mathbf{A} \in \mathbb{R}^{p \times p}$. According to (8), we can see that the search direction \mathbf{P}_k defined in (7) is induced by the metric $\|\cdot\|_{\mathbf{M}_k}$. Such search direction enables the algorithm to achieve fast convergence because of the second-order information incorporated from \mathbf{M}_k .

Unlike Problem (5), however, the closed-form solution for Problem (8) is not available because of the metric $\|\cdot\|_{\mathbf{M}_k}$. Though there are many iterative methods for solving the quadratic program (8) such as active set and interior-point methods, the procedure can be very computationally challenging for large-scale problems. To ease the computational burden, we replace the metric $\|\cdot\|_{\mathbf{M}_k}$ in (8) by the Frobenius norm, and obtain

$$\underset{\mathbf{X} \in \Omega}{\text{minimize}} \|\mathbf{X} - \mathbf{X}_k + \gamma_k \mathbf{P}_k\|_{\text{F}}^2. \quad (9)$$

Then we can get the closed-form solution of Problem (9), and establish the next iterate as follows,

$$\mathbf{X}_{k+1} = \mathcal{P}_{\Omega}(\mathbf{X}_k - \gamma_k \mathbf{P}_k), \quad (10)$$

where \mathbf{P}_k denotes the search direction defined in (7).

Remark 3.1. We call the iterate (10) as the two-metric projection method because two different metrics are adopted, *i.e.*, the search direction \mathbf{P}_k induced by the metric of the quadratic norm $\|\cdot\|_{\mathbf{M}_k}$, and the projection \mathcal{P}_{Ω} with respect to the metric of the Frobenius norm. Such method has the advantage of fast convergence by incorporating second-order information when constructing the search direction \mathbf{P}_k , while maintaining the computational efficiency of the projection \mathcal{P}_{Ω} to handle the constraints.

The iterate (10) requires the computation of the search direction \mathbf{P}_k as defined in (7). We note that, a straightforward implementation either relies on the inverse of \mathbf{M}_k whose dimension is $p^2 \times p^2$ or on solving a system of linear equations of the same dimension, of which the computation and memory costs are prohibitive in high-dimensional problems.

If we adopt \mathbf{M}_k as the exact Hessian matrix, then \mathbf{P}_k is the Newton direction and the iterate (10) can be viewed as a natural adaptation of the unconstrained Newton's method. Interestingly, we can exploit the structure of the Hessian, and reduce the computation and memory costs significantly as follows. By calculation, we obtain that the Hessian matrix of Problem (1) has the following special form,

$$\mathbf{H}_k = \mathbf{X}_k^{-1} \otimes \mathbf{X}_k^{-1}, \quad (11)$$

where \otimes denotes the Kronecker product. Following from the property of Kronecker product, we establish the following lemma, which is proved in Appendix A.5.

Lemma 3.2. *If \mathbf{M}_k is defined as the Hessian matrix \mathbf{H}_k in (11), then the search direction \mathbf{P}_k defined in (7) can be written as*

$$\mathbf{P}_k = \mathbf{X}_k \nabla f(\mathbf{X}_k) \mathbf{X}_k.$$

It is observed that the computation of \mathbf{P}_k from Lemma 3.2 only involves the gradient calculation and matrix multiplications, of which the computation and memory costs are considerably reduced compared to the straightforward implementation.

Unfortunately, the iterate (10) using the Newton direction \mathbf{P}_k from Lemma 3.2 cannot be guaranteed to converge to the minimizer because it may not be a descent iteration. More specifically, it may happen that the current iterate, which is on the boundary but not a minimizer, fails to decrease the value of the objective for an arbitrary step size, which is further demonstrated by our numerical results in Figure 2 in Section 5.1. Similar observations have also been reported in Bertsekas (1982, 2016); Kim et al. (2007).

In what follows, we construct an approximate Newton direction that can be computed efficiently and implemented easily, while it ensures convergence to the minimizer.

3.1 Identifying the Sets of *Restricted* and *Free* Variables

In order to guarantee the iterate (10) to converge to the minimizer, we partition the variables into two groups in each iteration, *i.e.*, *restricted* and *free* variables, and update the two groups separately. The *restricted* variables are directly set as zero according to the gradient information, while the *free* variables are updated along the constructed approximate Newton direction. Our variable partitioning scheme is as follows.

We first define a set $\mathcal{T}(\mathbf{X}, \epsilon)$ with respect to $\mathbf{X} \in \mathbb{R}^{p \times p}$ and $\epsilon \in \mathbb{R}_+$,

$$\mathcal{T}(\mathbf{X}, \epsilon) := \left\{ (i, j) \in [p]^2 \mid -\epsilon \leq X_{ij} \leq 0, [\nabla f(\mathbf{X})]_{ij} < 0 \right\}, \quad (12)$$

where $\nabla f(\mathbf{X})$ is the gradient in Problem (1), and $[p]^2$ denotes the set $\{1, \dots, p\} \times \{1, \dots, p\}$. Note that for each $\mathbf{X} \in \mathcal{M}^p$, (i, j) must be the index of an off-diagonal element if $(i, j) \in \mathcal{T}(\mathbf{X}, \epsilon)$. At the $(k+1)$ -th iteration, we identify the set of *restricted* variables based on \mathbf{X}_k as follows,

$$\mathcal{I}_k := \mathcal{T}(\mathbf{X}_k, \epsilon_k) \cup \mathcal{E}, \quad (13)$$

where \mathcal{E} is the disconnectivity set in Problem (1), and ϵ_k is a small positive scalar. For any $(i, j) \in \mathcal{T}(\mathbf{X}_k, \epsilon_k)$, X_{ij} in the next iterate is likely to be outside the feasible set (*i.e.*, $X_{ij} > 0$) if we remove the projection \mathcal{P}_Ω , because it is close to zero and moves towards the positive direction if using the negative of the gradient as the search direction. For any $(i, j) \in \mathcal{E}$, Problem (1) imposes X_{ij} to be zero. Therefore, we restrict all the *restricted* variables to be zero in the next iterate (more details can be found in Section 3.2).

To establish the theoretical convergence of our algorithm, we specify the positive scalar ϵ_k in (13) as

$$\epsilon_k := \min \left(2(1 - \alpha)m^2 \left\| [\nabla f(\mathbf{X}_k)]_{\mathcal{T}_\delta \setminus \mathcal{E}} \right\|_{\min}, \delta \right), \quad (14)$$

where m is some positive constant (defined in Lemma A.1), $\alpha \in (0, 1)$ is a parameter used in the backtracking line search, \mathcal{T}_δ denotes the set $\mathcal{T}(\mathbf{X}_k, \delta)$, and δ is a user-defined parameter that is required to be bounded by

$$0 < \delta < \min_{(i,j) \in \text{supp}(\mathbf{X}^*)} |[\mathbf{X}^*]_{ij}|, \quad (15)$$

where \mathbf{X}^* is the minimizer of Problem (1). To guarantee that Condition (15) holds, we can set a sufficiently small positive δ . In this case, ϵ_k in (14) is almost equal to δ . Therefore, from an implementation perspective, we can directly set a very small positive ϵ_k to avoid the estimation of m , and the algorithm always works well in practice.

The set of *free* variables \mathcal{I}_k^c is defined by the complement of the set of *restricted* variables \mathcal{I}_k . Our proposed algorithm updates the *free* and *restricted* variables separately as shown in Section 3.2. The theoretical results in Section 4 show that our proposed variable partitioning scheme enables $\{\mathcal{I}_k^c\}$ to converge to the support of the minimizer of Problem (1), which in turn validates the constructions of the sets \mathcal{I}_k and \mathcal{I}_k^c .

3.2 Computing the Approximate Newton Direction

It is often the case that computing the (approximate) Newton direction requires significantly more computation than computing the gradient. However, in this paper, we manage to construct an approximate Newton direction that has the same computational complexity as the gradient.

We start by partitioning \mathbf{X}_k into two groups, *restricted* group $[\mathbf{X}_k]_{\mathcal{I}_k}$ and *free* group $[\mathbf{X}_k]_{\mathcal{I}_k^c}$, where $[\mathbf{X}_k]_{\mathcal{I}_k} \in \mathbb{R}^{|\mathcal{I}_k|}$ and $[\mathbf{X}_k]_{\mathcal{I}_k^c} \in \mathbb{R}^{|\mathcal{I}_k^c|}$ denote two vectors containing all the elements of \mathbf{X}_k in the sets \mathcal{I}_k and \mathcal{I}_k^c , respectively. Without loss of generality, we assume that $\text{vec}(\mathbf{X}_k)$ and $\text{vec}(\mathbf{P}_k)$ can be partitioned as follows,

$$\text{vec}(\mathbf{X}_k) = \begin{bmatrix} [\mathbf{X}_k]_{\mathcal{I}_k^c} \\ [\mathbf{X}_k]_{\mathcal{I}_k} \end{bmatrix}, \quad \text{and} \quad \text{vec}(\mathbf{P}_k) = \begin{bmatrix} [\mathbf{P}_k]_{\mathcal{I}_k^c} \\ [\mathbf{P}_k]_{\mathcal{I}_k} \end{bmatrix}. \quad (16)$$

To compute the search direction \mathbf{P}_k defined in (7) efficiently, we propose the construction of \mathbf{M}_k^{-1} as

$$\mathbf{M}_k^{-1} = \begin{bmatrix} [\mathbf{M}_k^{-1}]_{\mathcal{I}_k^c \mathcal{I}_k^c} & [\mathbf{M}_k^{-1}]_{\mathcal{I}_k^c \mathcal{I}_k} \\ [\mathbf{M}_k^{-1}]_{\mathcal{I}_k \mathcal{I}_k^c} & [\mathbf{M}_k^{-1}]_{\mathcal{I}_k \mathcal{I}_k} \end{bmatrix} = \begin{bmatrix} [\mathbf{H}_k^{-1}]_{\mathcal{I}_k^c \mathcal{I}_k^c} & \mathbf{0} \\ \mathbf{0} & \mathbf{D}_k \end{bmatrix}, \quad (17)$$

where $\mathbf{D}_k \in \mathbb{R}^{|\mathcal{I}_k| \times |\mathcal{I}_k|}$ is a positive definite diagonal matrix, and $[\mathbf{H}_k^{-1}]_{\mathcal{I}_k^c \mathcal{I}_k^c} \in \mathbb{R}^{|\mathcal{I}_k^c| \times |\mathcal{I}_k^c|}$ is a principal submatrix of \mathbf{H}_k^{-1} keeping rows and columns indexed by \mathcal{I}_k^c , in which \mathbf{H}_k is the Hessian matrix at \mathbf{X}_k . We highlight that the construction of \mathbf{M}_k^{-1} in (17) is the key step in defining the search direction, which makes the computation and memory costs comparable to first-order methods, while incorporating the second-order information sufficiently.

We first construct the search direction \mathbf{P}_k over the *restricted* set \mathcal{I}_k , and present the iterate $[\mathbf{X}_{k+1}]_{\mathcal{I}_k}$. Following from (7) and (17), we know that the search direction $[\mathbf{P}_k]_{\mathcal{I}_k}$ is defined as $\mathbf{D}_k [\nabla f(\mathbf{X}_k)]_{\mathcal{I}_k}$. Since \mathbf{D}_k is a diagonal matrix, we can rewrite $[\mathbf{P}_k]_{\mathcal{I}_k}$ as

$$[\mathbf{P}_k]_{\mathcal{I}_k} = [\tilde{\mathbf{D}}_k \odot \nabla f(\mathbf{X}_k)]_{\mathcal{I}_k},$$

where \odot denotes the entry-wise product, and $\tilde{\mathbf{D}}_k$ is a $p \times p$ matrix, in which the elements $[\tilde{\mathbf{D}}_k]_{ij}$ for $(i, j) \in \mathcal{I}_k$ are from the diagonal elements of \mathbf{D}_k , and zeros for $(i, j) \in \mathcal{I}_k^c$.

For ease of presentation, by a slight abuse of notation, we write $\mathcal{P}_\Omega([\mathbf{A}]_{\mathcal{I}_k})$ for $[\mathcal{P}_\Omega(\mathbf{A})]_{\mathcal{I}_k}$. Then one has the iterate:

$$[\mathbf{X}_{k+1}]_{\mathcal{I}_k} = \mathcal{P}_\Omega\left([\mathbf{X}_k]_{\mathcal{I}_k} - \gamma_k [\tilde{\mathbf{D}}_k \odot \nabla f(\mathbf{X}_k)]_{\mathcal{I}_k}\right). \quad (18)$$

For each $(i, j) \in \mathcal{I}_k \setminus \mathcal{E}$, by setting

$$[\tilde{\mathbf{D}}_k]_{ij} = \frac{\epsilon_k}{\gamma_k |\nabla f(\mathbf{X}_k)_{ij}|},$$

we obtain $[\mathbf{X}_{k+1}]_{ij} = 0$, which follows from the definition of \mathcal{P}_Ω in (3). For each $(i, j) \in \mathcal{E}$, we also have $[\mathbf{X}_{k+1}]_{ij} = 0$. Note that all the indexes in \mathcal{I}_k correspond to the off-diagonal elements. To sum up, we have

$$[\mathbf{X}_{k+1}]_{\mathcal{I}_k} = \mathbf{0}. \quad (19)$$

We highlight that we can directly set $[\mathbf{X}_{k+1}]_{\mathcal{I}_k} = \mathbf{0}$ instead of computing $[\mathbf{X}_{k+1}]_{\mathcal{I}_k}$ according to (18) with an explicit $\tilde{\mathbf{D}}_k$.

Next, we compute the approximate Newton direction \mathbf{P}_k over the *free* set \mathcal{I}_k^c , and present the iterate $[\mathbf{X}_{k+1}]_{\mathcal{I}_k^c}$. We first define a projection $\mathcal{P}_{\mathcal{I}_k^c}(\mathbf{A})$ as follows,

$$[\mathcal{P}_{\mathcal{I}_k^c}(\mathbf{A})]_{ij} = \begin{cases} A_{ij} & \text{if } (i, j) \in \mathcal{I}_k^c, \\ 0 & \text{otherwise.} \end{cases} \quad (20)$$

Based on the well-designed gradient scaling matrix in (17), the corresponding approximate Newton direction can be computed efficiently as shown in the following lemma, which is proved in Section A.6.

Lemma 3.3. *If \mathbf{M}_k is defined by (17), then the search direction \mathbf{P}_k defined in (7) over \mathcal{I}_k^c can be written as*

$$[\mathbf{P}_k]_{\mathcal{I}_k^c} = [\mathbf{X}_k \mathcal{P}_{\mathcal{I}_k^c}(\nabla f(\mathbf{X}_k)) \mathbf{X}_k]_{\mathcal{I}_k^c}. \quad (21)$$

We observe that the computation costs of the search directions in Lemmas 3.2 and 3.3 are almost the same. However, our constructed search direction in Lemma 3.3 ensures the algorithm to converge to the minimizer of Problem (1), which is shown in Section 4.1.

By using the search direction $[\mathbf{P}_k]_{\mathcal{I}_k^c}$ from Lemma 3.3, we update the iterate \mathbf{X}_{k+1} over \mathcal{I}_k^c as follows,

$$[\mathbf{X}_{k+1}]_{\mathcal{I}_k^c} = \mathcal{P}_\Omega \left([\mathbf{X}_k]_{\mathcal{I}_k^c} - \gamma_k [\mathbf{X}_k \mathcal{P}_{\mathcal{I}_k^c} (\nabla f(\mathbf{X}_k)) \mathbf{X}_k]_{\mathcal{I}_k^c} \right). \quad (22)$$

To conclude, we update the *restricted* variables $[\mathbf{X}_{k+1}]_{\mathcal{I}_k}$ and *free* variables $[\mathbf{X}_{k+1}]_{\mathcal{I}_k^c}$ in each iteration according to (19) and (22), respectively.

3.3 Computing the Step Size

After computing the approximate Newton direction, we update the *free* variables $[\mathbf{X}_{k+1}]_{\mathcal{I}_k^c}$ by (22) with a step size $\gamma_k \in (0, 1]$. We select the step size via an Armijo-like rule that ensures the global convergence of the proposed algorithm.

More specifically, we try the step size $\gamma_k \in \{\beta^0, \beta^1, \beta^2, \dots\}$, where $\beta \in (0, 1)$ is a positive constant, until we find the smallest $m \in \mathbb{N}$ such that the next iterate \mathbf{X}_{k+1} with $\gamma_k = \beta^m$ is positive definite, and leads to a sufficient decrease of the objective function value:

$$f(\mathbf{X}_{k+1}) \leq f(\mathbf{X}_k) - \alpha \beta^m \left\langle [\nabla f(\mathbf{X}_k)]_{\mathcal{I}_k^c}, [\mathbf{P}_k]_{\mathcal{I}_k^c} \right\rangle - \alpha \left\langle [\nabla f(\mathbf{X}_k)]_{\mathcal{I}_k^c}, [\mathbf{X}_k]_{\mathcal{I}_k} - [\mathbf{X}_{k+1}]_{\mathcal{I}_k} \right\rangle,$$

where $\alpha \in (0, 1)$ is a positive scalar. The backtracking line search condition above is a variant of the Armijo rule, and this condition can guarantee that the iterate will not terminate until it reaches the minimizer of Problem (1) (more details can be found in the proof of Theorem 4.3). Note that the positive definiteness of \mathbf{X}_{k+1} can be verified when we compute the Cholesky factorization for evaluating the objective function. The proposed algorithm is summarized in Algorithm 1.

3.4 Computational Complexity

It is observed in (21) that, to compute the approximate Newton direction, our algorithm needs to compute the gradient $\nabla f(\mathbf{X}_k)$, two matrix multiplications, and one projection, whose computational costs are $O(p^3)$, $O(p^3)$, and $O(p^2)$, respectively. Therefore, the computational complexity of our proposed algorithm is $O(p^3)$ in computing the search direction, which is the same as that of the projected gradient method. In practice, because our algorithm exploits the benefits of the second-order information when defining the search direction, it shows a faster convergence than the projected gradient method.

The Cholesky factorization, which requires $O(p^3)$ operations, is needed in computing the objective function value of Problem (1), and that dominates the computational cost in backtracking line search. Note that the backtracking line search is typically also needed for other gradient or Newton-based algorithms to adaptively choose the step size.

In summary, the overall computational complexity of our proposed algorithm is $O(p^3)$ per iteration. Recall that BCD-type algorithms (Slawski and Hein, 2015; Pavez and Ortega, 2016; Egilmez et al., 2017) require $O(p^4)$ operations in each cycle, and the projected quasi-Newton with L-BFGS (Kim et al., 2010) requires $O((m+p)p^2)$ operations per iteration, where m is the number of iterations stored for approximating the inverse Hessian. In addition, our algorithm requires $O(p^2)$ memory that is the same as those of the projected gradient method and BCD-type algorithms (Slawski and Hein, 2015; Pavez and Ortega, 2016; Egilmez et al., 2017), while the projected quasi-Newton with L-BFGS (Kim et al., 2010) requires $O(mp^2)$ memory.

4 Theoretical Results

In this section, we first prove that our proposed algorithm converges to the minimizer of Problem (1) and the set of *free* variables converges to the support of the minimizer. The convergence rate of our algorithm is also analyzed. Then, we establish the support recovery consistency of the minimizer of Problem (1) without requiring the *incoherence* condition.

Algorithm 1 Fast Projected Newton-like (FPN) algorithm

- 1: **Input:** Sample covariance matrix \mathbf{S} , regularization parameter λ_{ij} , α , and β ;
- 2: **for** $k = 0, 1, 2, \dots$ **do**
- 3: Identify the *restricted* set \mathcal{I}_k and *free* set \mathcal{I}_k^c according to (13);
- 4: Compute the approximate Newton direction over the set \mathcal{I}_k^c :

$$[\mathbf{P}_k]_{\mathcal{I}_k^c} = \left[\mathbf{X}_k \mathcal{P}_{\mathcal{I}_k^c}(\nabla f(\mathbf{X}_k)) \mathbf{X}_k \right]_{\mathcal{I}_k^c};$$

5: $m \leftarrow 0$;

6: **repeat**

7: Update \mathbf{X}_{k+1} : $[\mathbf{X}_{k+1}]_{\mathcal{I}_k} = \mathbf{0}$, and $[\mathbf{X}_{k+1}]_{\mathcal{I}_k^c} = \mathcal{P}_\Omega \left([\mathbf{X}_k]_{\mathcal{I}_k^c} - \beta^m [\mathbf{P}_k]_{\mathcal{I}_k^c} \right)$;

8: $m \leftarrow m + 1$;

9: **until** $\mathbf{X}_{k+1} \succ \mathbf{0}$, and

$$f(\mathbf{X}_{k+1}) \leq f(\mathbf{X}_k) - \alpha \beta^m \left\langle [\nabla f(\mathbf{X}_k)]_{\mathcal{I}_k^c}, [\mathbf{P}_k]_{\mathcal{I}_k^c} \right\rangle - \alpha \left\langle [\nabla f(\mathbf{X}_k)]_{\mathcal{I}_k}, [\mathbf{X}_k]_{\mathcal{I}_k} - [\mathbf{X}_{k+1}]_{\mathcal{I}_k} \right\rangle.$$

10: **end for**

4.1 Convergence Analysis

To establish the theoretical convergence of Algorithm 1, we first show that the minimizer of Problem (1) is unique in the following proposition, proved in Appendix A.1.

Proposition 4.1. *Suppose the sample covariance matrix \mathbf{S} in Problem (1) has strictly positive diagonal elements. Then there exists a unique minimizer of (1), and a point $\mathbf{X}^* \in \mathcal{M}^p$ is the minimizer if and only if it satisfies*

$$[\mathbf{X}^*]_{ij} = 0 \quad \forall (i, j) \in \mathcal{E}, \quad [\nabla f(\mathbf{X}^*)]_{\mathcal{V} \setminus \mathcal{E}} \leq \mathbf{0}, \quad \text{and} \quad [\nabla f(\mathbf{X}^*)]_{\mathcal{V}^c} = \mathbf{0}, \quad (23)$$

where $\mathcal{V} = \left\{ (i, j) \in [p]^2 \mid [\mathbf{X}^*]_{ij} = 0 \right\}$.

Note that the sample covariance matrix is constructed by $\mathbf{S} = \frac{1}{n} \sum_{i=1}^n \mathbf{y}^{(i)} (\mathbf{y}^{(i)})^\top$, where $\mathbf{y}^{(1)}, \dots, \mathbf{y}^{(n)} \in \mathbb{R}^p$ are independent observations under a multivariate Gaussian distribution with MTP₂ constraints. We can see if some diagonal element S_{jj} is zero, then the j -th element of $\mathbf{y}^{(i)}$ must be zero for every $i \in [p]$, which holds with probability zero. Consequently, the condition that the diagonal elements of \mathbf{S} are strictly positive holds with probability one. Therefore, in the rest of this paper, the sample covariance matrix is assumed to have strictly positive diagonal elements.

Assumption 4.2. Let \mathbf{X}^* be the minimizer of Problem (1). The gradient of the objective function f at \mathbf{X}^* satisfies

$$[\nabla f(\mathbf{X}^*)]_{ij} < 0, \quad \forall (i, j) \in \mathcal{V} \setminus \mathcal{E},$$

where $\mathcal{V} = \left\{ (i, j) \in [p]^2 \mid [\mathbf{X}^*]_{ij} = 0 \right\}$, and \mathcal{E} is the disconnectivity set.

In Assumption 4.2, we impose an assumption on the minimizer \mathbf{X}^* that $[\nabla f(\mathbf{X}^*)]_{ij}$ is strictly negative for any $(i, j) \in \mathcal{V} \setminus \mathcal{E}$. This assumption is very mild, because Proposition 4.1 shows that the minimizer \mathbf{X}^* must satisfy $[\nabla f(\mathbf{X}^*)]_{ij} \leq 0$ for each $(i, j) \in \mathcal{V} \setminus \mathcal{E}$. The only difference is that we need the inequality to be strict to establish the following theorem.

Theorem 4.3. *Under Assumption 4.2, the sequence $\{\mathbf{X}_k\}$ generated by Algorithm 1 converges to the minimizer \mathbf{X}^* of Problem (1), with $\{f(\mathbf{X}_k)\}$ monotonically decreasing. Moreover, there exists some $k_o \in \mathbb{N}_+$ such that*

$$\mathcal{I}_k^c = \text{supp}(\mathbf{X}^*), \quad \forall k \geq k_o.$$

In other words, for any $k \geq k_o$, the set of free variables is consistent with the support of \mathbf{X}^ .*

Theorem 4.3, proved in Appendix A.2, shows that the proposed algorithm generates a sequence $\{\mathbf{X}_k\}$ that converges to the unique minimizer of Problem (1) and the objective function value monotonically decreases. Furthermore, the set \mathcal{I}_k^c constructed by our variable partitioning scheme can exactly identify the support of the minimizer \mathbf{X}^* in a finite number of iterations, which in turn validates the constructions of the sets \mathcal{I}_k and \mathcal{I}_k^c .

In what follows, we discuss the convergence rate of the proposed algorithm. Newton-type methods may enjoy an asymptotic superlinear convergence rate, *i.e.*, the ratio of successive residuals tends to zero as the number of iterations increases to infinity. For unconstrained optimization problems, the necessary and sufficient condition on the search direction to achieve the superlinear rate of convergence has been well studied. Consider the search direction \mathbf{P}_k as $\text{vec}(\mathbf{P}_k) = \mathbf{R}_k^{-1} \text{vec}(\nabla f(\mathbf{X}_k))$, where \mathbf{R}_k^{-1} is a gradient scaling matrix. Then the necessary and sufficient condition for achieving the superlinear convergence rate is as follows (Nocedal and Wright, 2006),

$$\lim_{k \rightarrow \infty} \frac{\|(\mathbf{R}_k - \nabla^2 f(\mathbf{X}^*))\mathbf{p}_k\|}{\|\mathbf{p}_k\|} = 0, \quad (24)$$

where \mathbf{p}_k denotes $\text{vec}(\mathbf{P}_k)$, \mathbf{X}^* is the minimizer of the optimization problem, and $\nabla^2 f(\mathbf{X}^*)$ is positive definite. To obtain the superlinear convergence rate, the sequence $\{\mathbf{R}_k\}$ must increasingly approximate $\nabla^2 f(\mathbf{X}^*)$ along the search direction \mathbf{p}_k .

For constrained problems, Bertsekas (1982) showed that the iterate of the projected Newton algorithm can be reduced to an iterate of an unconstrained minimization algorithm on the subspace corresponding to the support of \mathbf{X}^* after a finite number of iterations. Though the projected Newton method proposed in Bertsekas (1982) proves to have the asymptotic superlinear convergence rate, it needs to calculate the inverse of some principle submatrix of the Hessian, in order to obtain the search direction. Note that the Hessian matrix has the dimension $p^2 \times p^2$ for Problem (1), resulting in prohibitive computation and memory costs for the method proposed in Bertsekas (1982).

To overcome this issues, we construct a well-designed approximate Newton direction in Section 3.2 that can be computed efficiently and implemented easily. To analyze its convergence rate, we rewrite the iterate (10) as an iterate for solving an unconstrained optimization problem. For any $k \geq k_o$, we can remove the projection \mathcal{P}_Ω , and use the iterate \mathbf{X}_{k+1} as follows (more details can be found in the proof of Corollary 4.4),

$$[\mathbf{X}_{k+1}]_{\mathcal{I}_k} = \mathbf{0}, \quad \text{and} \quad [\mathbf{X}_{k+1}]_{\mathcal{I}_k^c} = [\mathbf{X}_k]_{\mathcal{I}_k^c} - \gamma_k [\mathbf{P}_k]_{\mathcal{I}_k^c}. \quad (25)$$

Therefore, we can focus the iterate over \mathcal{I}_k^c . Together with (7) and (17), we obtain

$$[\mathbf{X}_{k+1}]_{\mathcal{I}_k^c} = [\mathbf{X}_k]_{\mathcal{I}_k^c} - \gamma_k \mathbf{R}_k^{-1} [\nabla f(\mathbf{X}_k)]_{\mathcal{I}_k^c}, \quad (26)$$

where the gradient scaling matrix $\mathbf{R}_k^{-1} = [\mathbf{H}_k^{-1}]_{\mathcal{I}_k^c \mathcal{I}_k^c}$, which is positive definite, and \mathbf{R}_k admits

$$\mathbf{R}_k = [\mathbf{H}_k]_{\mathcal{I}_k^c \mathcal{I}_k^c} - [\mathbf{H}_k]_{\mathcal{I}_k^c \mathcal{I}_k} [\mathbf{H}_k]_{\mathcal{I}_k \mathcal{I}_k}^{-1} [\mathbf{H}_k]_{\mathcal{I}_k \mathcal{I}_k^c}^\top. \quad (27)$$

We check that the matrix \mathbf{R}_k does not satisfy the condition (24), because the term $[\mathbf{H}_k]_{\mathcal{I}_k^c \mathcal{I}_k} [\mathbf{H}_k]_{\mathcal{I}_k \mathcal{I}_k}^{-1} [\mathbf{H}_k]_{\mathcal{I}_k \mathcal{I}_k^c}^\top$ does not tend to be zero or orthogonal to the search direction as $k \rightarrow \infty$. Thus, our algorithm does not converge superlinearly. However, the term $[\mathbf{H}_k]_{\mathcal{I}_k^c \mathcal{I}_k} [\mathbf{H}_k]_{\mathcal{I}_k \mathcal{I}_k}^{-1} [\mathbf{H}_k]_{\mathcal{I}_k \mathcal{I}_k^c}^\top$ usually contributes significantly

less than the term $[\mathbf{H}_k]_{\mathcal{I}_k^c \mathcal{I}_k^c}$. For example, if the learned graph is a star graph with p nodes, then $[\mathbf{H}_k]_{\mathcal{I}_k^c \mathcal{I}_k} [\mathbf{H}_k]_{\mathcal{I}_k \mathcal{I}_k}^{-1} [\mathbf{H}_k]_{\mathcal{I}_k^c \mathcal{I}_k}^\top$ with the dimension $(3p - 2) \times (3p - 2)$ always has $p + 1$ zero eigenvalues as $k \rightarrow \infty$; if $|\mathcal{I}_k^c|$ is considerably larger than $|\mathcal{I}_k|$, then $[\mathbf{H}_k]_{\mathcal{I}_k^c \mathcal{I}_k} [\mathbf{H}_k]_{\mathcal{I}_k \mathcal{I}_k}^{-1} [\mathbf{H}_k]_{\mathcal{I}_k^c \mathcal{I}_k}^\top$ also has many zero eigenvalues. Note that $[\mathbf{H}_k]_{\mathcal{I}_k^c \mathcal{I}_k} [\mathbf{H}_k]_{\mathcal{I}_k \mathcal{I}_k}^{-1} [\mathbf{H}_k]_{\mathcal{I}_k^c \mathcal{I}_k}^\top$ is a positive semidefinite matrix. Therefore, the positive definite \mathbf{R}_k usually approximates well the positive definite $[\mathbf{H}_k]_{\mathcal{I}_k^c \mathcal{I}_k^c}$, and thus the scaling matrix \mathbf{R}_k^{-1} in (26) can improve the convergence rate as illustrated below. Define m_k and M_k as the smallest and largest eigenvalues of $\mathbf{R}_k^{-\frac{1}{2}} [\mathbf{H}_k]_{\mathcal{I}_k^c \mathcal{I}_k^c} \mathbf{R}_k^{-\frac{1}{2}}$, respectively. The following corollary is a direct extension of the result in Bertsekas (2016).

Corollary 4.4. *Under Assumption 4.2, the sequence $\{\mathbf{X}_k\}$ generated by Algorithm 1 satisfies*

$$\limsup_{k \rightarrow \infty} \frac{\|\mathbf{X}_{k+1} - \mathbf{X}^*\|_{\mathbf{M}_k}^2}{\|\mathbf{X}_k - \mathbf{X}^*\|_{\mathbf{M}_k}^2} \leq \limsup_{k \rightarrow \infty} \left(1 - \min \left(m_k, \frac{2(1 - \alpha)\beta m_k}{M_k} \right) \right)^2.$$

We can see in Corollary 4.4 that the convergence rate depends on the condition number m_k/M_k of $\mathbf{R}_k^{-\frac{1}{2}} [\mathbf{H}_k]_{\mathcal{I}_k^c \mathcal{I}_k^c} \mathbf{R}_k^{-\frac{1}{2}}$. If we replace the matrix \mathbf{R}_k by an identity matrix, (*i.e.*, turn the iterate into the projected gradient method), then the convergence rate will depend on the condition number of $[\mathbf{H}_k]_{\mathcal{I}_k^c \mathcal{I}_k^c}$. We note that the condition number of $\mathbf{R}_k^{-\frac{1}{2}} [\mathbf{H}_k]_{\mathcal{I}_k^c \mathcal{I}_k^c} \mathbf{R}_k^{-\frac{1}{2}}$ could be larger than that of $[\mathbf{H}_k]_{\mathcal{I}_k^c \mathcal{I}_k^c}$, since \mathbf{R}_k could approximate $[\mathbf{H}_k]_{\mathcal{I}_k^c \mathcal{I}_k^c}$ well. Therefore, the gradient scaling matrix \mathbf{R}_k^{-1} , *i.e.*, $[\mathbf{H}_k^{-1}]_{\mathcal{I}_k^c \mathcal{I}_k^c}$, leads our proposed projected Newton-like method to converge faster than the projected gradient method, while they require the same orders of computation and memory costs.

4.2 Support Recover Consistency

In this subsection, we establish the support recover consistency of the minimizer \mathbf{X}^* of Problem (1) without requiring the *incoherence* condition.

We start by the notation and assumption needed for establishing our theoretical results. Let $\Theta \in \mathcal{M}^p$ be the underlying precision matrix, whose support set $\text{supp}(\Theta)$ is

$$\mathcal{S} := \{(i, j) \in [p]^2 \mid \Theta_{ij} \neq 0\}.$$

The support set \mathcal{S} can be partitioned into two disjoint subsets, the indexes corresponding to the elements on the diagonal and off the diagonal, *i.e.*, $\mathcal{S} = \mathcal{S}_{\text{on}} \cup \mathcal{S}_{\text{off}}$, where

$$\mathcal{S}_{\text{on}} := \{(i, j) \in [p]^2 \mid \Theta_{ij} > 0, i = j\}, \text{ and } \mathcal{S}_{\text{off}} := \{(i, j) \in [p]^2 \mid \Theta_{ij} < 0, i \neq j\}.$$

Note that all the off-diagonal elements of Θ are nonpositive, and the elements on the diagonal are strictly positive, due to the fact that $\Theta \in \mathcal{M}^p$. Then we define

$$\mathcal{S}^c := \{(i, j) \in [p]^2 \mid \Theta_{ij} = 0\},$$

where all indexes in \mathcal{S}^c correspond to the off-diagonal elements. Let

$$\mathcal{S}' = \mathcal{S}^c \setminus \mathcal{E},$$

where \mathcal{E} is the disconnectivity set imposed in Problem (1), and we assume $\mathcal{E} \subseteq \mathcal{S}^c$.

Let d be the maximum number of nonzero elements in any row of Θ , which corresponds to the maximum degree of the underlying graph. Note that we include the diagonal elements of Θ when counting the degree, which can be viewed as the self-loop of each node.

We define two quantities that only depend on the underlying precision matrix,

$$K_\Sigma = \max_{i \in [p]} \sum_{j=1}^p |\Sigma_{ij}|, \quad \text{and} \quad K_H = \left\| (\mathbf{H}_{SS})^{-1} \right\|_\infty, \quad (28)$$

where Σ is the underlying covariance matrix, *i.e.*, $\Sigma = \Theta^{-1}$, and \mathbf{H}_{SS} is a $|\mathcal{S}| \times |\mathcal{S}|$ principle submatrix of \mathbf{H} , with both rows and columns indexed by \mathcal{S} , in which \mathbf{H} is the Hessian matrix at Θ , *i.e.*, $\mathbf{H} = \Theta^{-1} \otimes \Theta^{-1}$.

We collect the regularization weights λ_{ij} , $(i, j) \in [p]^2$, of Problem (1) into a matrix $\lambda \in \mathbb{R}^{p \times p}$. If we specify each weight as $\lambda_{ij} = C_{ij} \sqrt{\frac{\log p}{n}}$, then we have $\lambda = \sqrt{\frac{\log p}{n}} \mathbf{C}$, where \mathbf{C} contains all the parameters C_{ij} . Note that we do not impose the sparsity penalty on the diagonal elements of \mathbf{X} , therefore $C_{ij} = 0$ for any $i = j$.

Assumption 4.5. The nonzero off-diagonal elements of Θ satisfies

$$\min_{(i,j) \in \mathcal{S}_{\text{off}}} |\Theta_{ij}| > \frac{4}{3} K_H \|\lambda_{\mathcal{S}}\|_{\max},$$

where $\|\lambda_{\mathcal{S}}\|_{\max} = \max_{(i,j) \in \mathcal{S}} |\lambda_{ij}|$, in which λ_{ij} is the regularization weight in Problem (1).

Assumption 4.5 imposes a lower bound on the minimal absolute value of Θ over the set \mathcal{S}_{off} . This condition is mild because the regularization weight λ_{ij} in our theorem is taken with the order $\sqrt{\log p/n}$ that can be very small when the sample size n increases.

Theorem 4.6. Suppose the regularization weights in Problem (1) are specified as $\lambda = \sqrt{\frac{\log p}{n}} \mathbf{C}$ and satisfy

$$\frac{\|\mathbf{C}_{\mathcal{S}'}\|_{\min}}{\|\mathbf{C}_{\mathcal{S}}\|_{\max}} \geq 2 \left\| \mathbf{H}_{\mathcal{S}'\mathcal{S}} (\mathbf{H}_{SS})^{-1} \right\|_\infty, \quad (29)$$

and the sample covariance matrix \mathbf{S} satisfies

$$\|\Sigma - \mathbf{S}\|_{\max} \leq c_0 \sqrt{\frac{\log p}{n}}. \quad (30)$$

Under Assumption 4.5, if the sample size is lower bounded by $n \geq cd^2 \log p$, where $c = (4c_1 K_H K_\Sigma \max(4c_2 K_H K_\Sigma^2, 1))^2$, then the minimizer \mathbf{X}^* of Problem (1) recovers the support of the underlying precision matrix Θ correctly, *i.e.*,

$$\text{supp}(\mathbf{X}^*) = \text{supp}(\Theta),$$

where $c_0 = \frac{1}{6} \min(\|\mathbf{C}_{\mathcal{S}}\|_{\max}, \|\mathbf{C}_{\mathcal{S}'}\|_{\min})$, $c_1 = \|\mathbf{C}_{\mathcal{S}}\|_{\max}$, and $c_2 = \max\left(\frac{\|\mathbf{C}_{\mathcal{S}}\|_{\max}}{\|\mathbf{C}_{\mathcal{S}'}\|_{\min}}, 1\right)$.

Theorem 4.6, proved in Appendix A.4, establishes the support recovery consistency of the minimizer \mathbf{X}^* of Problem (1), implying that all the underlying graph edges associated with Θ can be identified through \mathbf{X}^* . We note that the deviation condition (30) holds with an overwhelming probability $1 - k_1 \exp(-k_2 \log p)$ for Gaussian observations, or the more general class of sub-Gaussian observations, where k_1 and k_2 are two positive constants. If we view the quantities K_H and K_Σ as constants, then the requirement on the sample size is $n \gtrsim d^2 \log p$, which has only logarithmic dependence on the number of nodes p .

Condition (29) depends on the parameters \mathbf{C} of the regularization weights. If some element Θ_{ij} in the underlying precision matrix is small or zero, then C_{ij} is expected to be large so as to impose a strong sparsity penalty on X_{ij} ; otherwise, C_{ij} is expected to be small. Therefore, we compute \mathbf{C} in an adaptive way based on an initial estimator \mathbf{X}_o . More specifically, we consider

$$C_{ij} = \psi(|[\mathbf{X}_o]_{ij}|), \quad \forall i \neq j, \quad (31)$$

where ψ is a monotonically decreasing function. For example, $\psi(x) = (x + \epsilon)^{-1}$, in which ϵ is a small positive scalar. We may consider the maximum likelihood estimator as \mathbf{X}_o , which is a consistent estimator and exists with only two observations. As the number of samples grows, $[\mathbf{X}_o]_{ij}$ will converge to zero for any $(i, j) \in \mathcal{S}'$, then the resulting C_{ij} will be large. In contrast, C_{ij} will become small for any $(i, j) \in \mathcal{S}$. Therefore, Condition (29) can always hold given a suitable function ψ and enough samples.

It is known that *incoherence* conditions are almost necessary for the ℓ_1 -norm based methods to be selection consistent (Zhao and Yu, 2006; Meinshausen and Bühlmann, 2006; Tropp, 2006; Ravikumar et al., 2011). For example, graphical lasso typically requires the *incoherence* condition, also known as the *irrepresentability* condition, on the underlying precision matrix Θ for support recovery consistency, which can be stated as follows (Ravikumar et al., 2011),

$$\left\| \left\| \mathbf{H}_{\mathcal{S}^c \mathcal{S}} (\mathbf{H}_{\mathcal{S}\mathcal{S}})^{-1} \right\| \right\|_{\infty} \leq 1 - \eta, \quad \text{for some } \eta \in (0, 1], \quad (32)$$

where \mathbf{H} is the Hessian at Θ , *i.e.*, $\mathbf{H} = \Theta^{-1} \otimes \Theta^{-1}$. We note that the *incoherence* condition (32) may not hold in practice and is not straightforward to interpret. However, the statements in Theorem 4.6 hold without assuming such condition on Θ , while we impose Condition (29) on regularization parameters instead, which can always hold as discussed above. Our results are consistent with previous results in linear regression models that the weighted ℓ_1 -regularized methods enjoy the variable selection consistency without requiring the *incoherence* condition (Zou, 2006).

5 Experimental Results

We conduct experiments on synthetic and real-world data to verify the performance of the proposed algorithm. All experiments were conducted on 2.10GHZ Xeon Gold 6152 machines with 80G RAM and Linux OS, and all compared methods were implemented in MATLAB.

The state-of-the-art methods for comparing the computational time in estimating sparse precision matrices under MTP_2 constraints include:

- BCD: block coordinate descent algorithm proposed in (Slawski and Hein, 2015), which updates a single column/row of the precision matrix at a time by solving a nonnegative quadratic program on the primal variable.
- optGL: block coordinate descent algorithm proposed in (Pavez and Ortega, 2016), which solves nonnegative quadratic programs on the dual variable.
- GGL: block coordinate descent algorithm proposed in (Egilmez et al., 2017), which solves nonnegative quadratic programs on the primal variable similar to BCD, but can handle disconnectivity constraints.
- PGD: projected gradient descent method with the backtracking line search, which is a baseline method. The iterate is formulated in (4).
- APGD: accelerated projected gradient algorithm (Nesterov, 1983, 2003) that employs an extrapolation step.
- PQN-LBFGS: projected quasi-Newton method that employs the limited-memory BFGS to approximate the inverse Hessian (Kim et al., 2010).

Note that all the state-of-the-art methods listed above can converge to the minimizer of Problem (1), and we focus on the comparisons of the computational time required for those methods. To that end, we report the relative error of the objective function value as a function of the run time, which is calculated by

$$|f(\mathbf{X}_k) - f(\mathbf{X}^*)| / |f(\mathbf{X}^*)|, \quad (33)$$

where f is the objective function of Problem (1), and \mathbf{X}^* is its minimizer. The \mathbf{X}^* is computed by running the state-of-the-art method GGL (Egilmez et al., 2017) until it converges to a point $\mathbf{X}_k \in \mathcal{M}^p$ satisfying

$$[\mathbf{X}_k]_{ij} = 0 \quad \forall (i, j) \in \mathcal{E}, \quad [\nabla f(\mathbf{X}_k)]_{\mathcal{A} \setminus \mathcal{E}} \leq \mathbf{0}, \quad \text{and} \quad \|\nabla f(\mathbf{X}^*)\|_{\mathcal{A}^c} \leq 10^{-8}, \quad (34)$$

where $\mathcal{A} := \{(i, j) \in [p]^2 \mid |[\mathbf{X}_k]_{ij}| \leq 10^{-8}\}$. Through the comparison with the sufficient and necessary conditions of the unique minimizer of Problem (1) presented in Proposition 4.1, we can see that any point \mathbf{X}_k satisfying the conditions (34) is very close to the minimizer. There is no additional computational cost for PGD, APGD, PQN-LBFGS and our proposed FPN in computing the relative error as shown in (33), because the objective function value has been evaluated in the backtracking line search in each iteration. The methods BCD, optGL, and GGL do not need to evaluate the objective function, and thus additional cost is needed in computing the relative error in (33) for comparisons. However, this cost can be almost ignored, since they compute the objective function value only after completing a cycle, and the number of cycles required for BCD, optGL, and GGL is considerably smaller than the number of iterations required for the other methods.

We set the regularization parameter λ_{ij} in Problem (1) as follows

$$\lambda_{ij} = \frac{\sigma}{|[\mathbf{X}_o]_{ij}| + \epsilon}, \quad \forall i \neq j, \quad (35)$$

where \mathbf{X}_o is some estimator, ϵ is set as 10^{-3} , and $\sigma > 0$ is the parameter to adjust the sparsity. The function in (35) is closely related to the re-weighted ℓ_1 -norm regularization (Candes et al., 2008; Liu and Ihler, 2011; Kumar et al., 2020), which is effective in enhancing the sparsity of the solution. We use the maximum likelihood estimator as \mathbf{X}_o , *i.e.*, the minimizer of Problem (1) without the sparsity regularization. Note that one may solve the maximum likelihood estimator with a relatively large tolerance to obtain a coarse estimator, and one may also explore other monotonically decreasing functions in (35). For PQN-LBFGS, we use the previous 50 updates to compute the search direction. For our proposed FPN, we set $\epsilon_k = 10^{-15}$ in (13) for identifying the set of *restricted* variables.

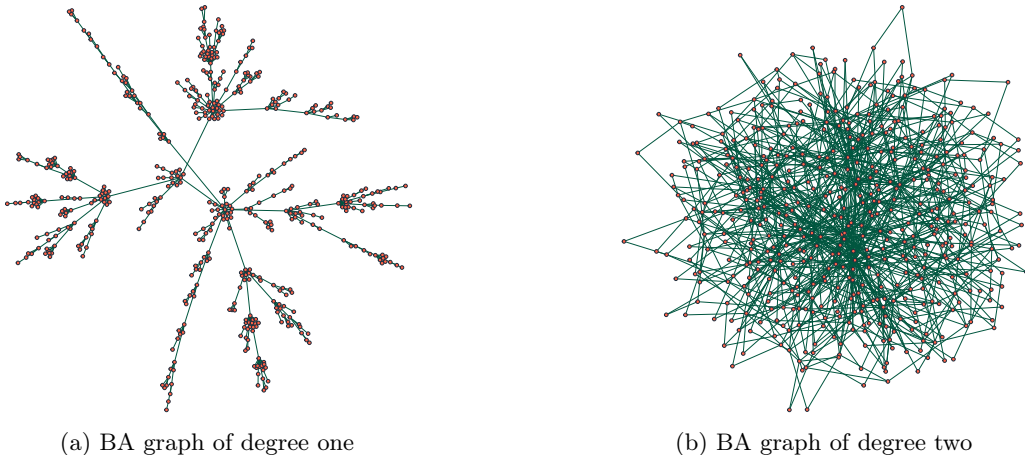


Figure 1: Illustration of the generated BA graph of degree one in (a), and BA graph of degree two in (b), both consisting of 500 nodes.

5.1 Synthetic Data

We first verify that our proposed algorithm converges to the minimizer of Problem (1), while the Newton direction from Lemma 3.2 fails to do it. Then we compare the computational time of different methods in solving Problem (1) for obtaining the minimizer. Finally, we present the successful support recovery of the minimizer of Problem (1) in experiments.

We generate independent samples $\mathbf{y}^{(1)}, \dots, \mathbf{y}^{(n)} \in \mathbb{R}^p$ from a multivariate Gaussian distribution with zero mean and precision matrix Θ , where $\Theta \in \mathcal{M}^p$ is the underlying precision matrix associated with a graph consisting of p nodes. Then the sample covariance matrix is constructed by $\mathbf{S} = \frac{1}{n} \sum_{i=1}^n \mathbf{y}^{(i)} (\mathbf{y}^{(i)})^\top$.

We consider Barabasi-Albert (BA) graphs (Barabási and Albert, 1999) as the model for the support of the underlying precision matrix. BA models play an important role in network science, which generate random scale-free networks using a *preferential attachment* mechanism such that new nodes tend to link to nodes that have higher degree in the evolution. Scale-free networks are well-suited to model the Internet, the world wide web, protein interaction networks, citation networks, and most social and online networks (Barabási and Albert, 1999). A BA graph of degree r indicates that each new node is connected to r existing nodes with a probability that is proportional to the number of edges that the existing nodes already have. In this paper, we generate BA graphs of degree r with $r = 1, 2$, as shown in Figure 1.

We assign a positive weight to each edge of a BA graph, and set a zero weight if two nodes are disconnected, where positive weights are uniformly sampled from $U(2, 5)$. As a result, we obtain a weighted adjacency matrix \mathbf{A} that contains all the graph weights. We adopt the procedures used in Slawski and Hein (2015) to generate the underlying precision matrix Θ . We first set

$$\tilde{\Theta} = \delta \mathbf{I} - \mathbf{A}, \quad \text{with } \delta = 1.05 \lambda_{\max}(\mathbf{A}), \quad (36)$$

where $\lambda_{\max}(\mathbf{A})$ denotes the largest eigenvalue of \mathbf{A} . We set $\Theta = \mathbf{D} \tilde{\Theta} \mathbf{D}$, where \mathbf{D} is a diagonal matrix chosen such that the covariance matrix Θ^{-1} has unit diagonal elements.

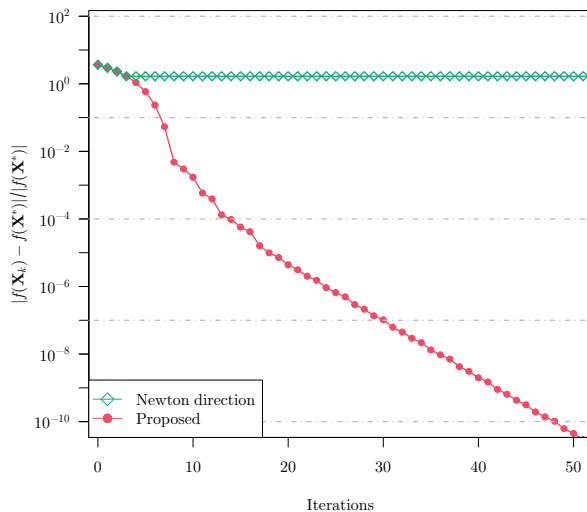


Figure 2: Comparisons of convergence of the proposed algorithm and the algorithm using the Newton direction from Lemma 3.2 on the data set of BA graph consisting of 500 nodes.

5.1.1 Comparisons of convergence

We compare the convergence of our proposed algorithm using the approximate Newton direction from Lemma 3.3 and the algorithm that adopts the Newton direction from Lemma 3.2 in iterate (10). It is observed in Figure 2 that our algorithm converges to the minimizer, which is consistent with our theoretical convergence results presented in Theorem 4.3. In contrast, Figure 2 shows that the objective function value of the algorithm using the Newton direction does not continue decreasing after 3 iterations. Note that the algorithm selects the step size by the Armijo rule, *i.e.*, the step size is repeatedly reduced until the next iterate leads to a decrease of the objective function. Therefore, the Newton direction from Lemma 3.2 cannot decrease the objective function value for any positive step size at fourth iteration, implying that it cannot be guaranteed to be a descent direction.

5.1.2 Comparisons of computational time

We compare the computational time of our algorithm with the state-of-the-art methods in estimating sparse precision matrices on synthetic data sets.

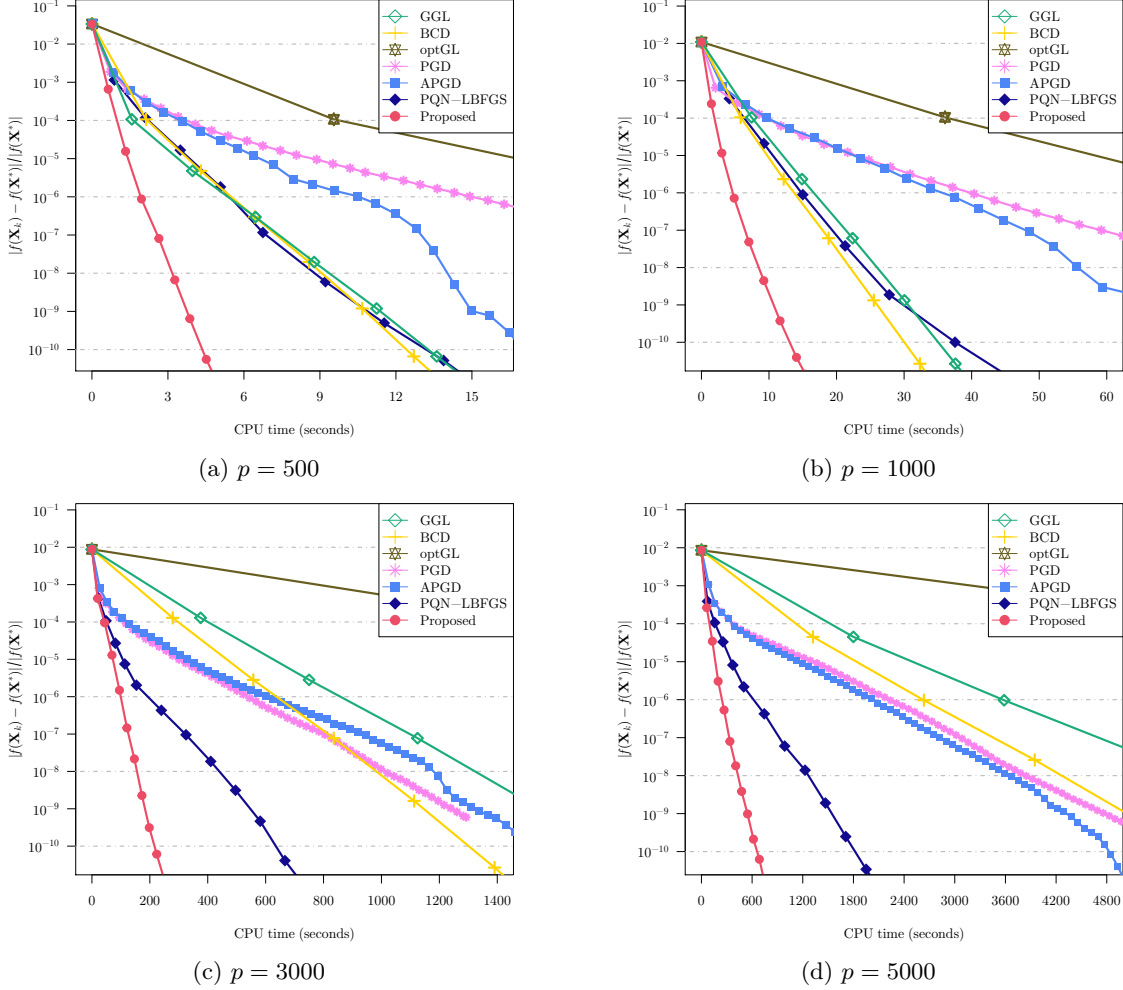


Figure 3: Relative errors of the objective function values versus time on synthetic data sets: BA graphs of degree one consisting of p nodes, (a) $p = 500$, (b) $p = 1000$, (c) $p = 3000$, and (d) $p = 5000$. The regularization parameter σ in (35) is chosen such that the minimizer \mathbf{X}^* has a close number of nonzero elements as compared to that of the underlying precision matrix Θ . All results are averaged over 10 realizations.

Figure 3 compares the computational time of different methods in solving Problem (1) on BA graphs of degree one. It is observed that our proposed FPN always takes significantly less time than all state-of-the-art methods to converge to the minimizer for the number of nodes ranging from 500 to 5000. We also observe that the methods BCD and GGL are efficient for the cases of 500 and 1000 nodes, where they are faster than PGD and APGD, and competitive with PQN-LBFGS. However, as the number of nodes p increases to 5000, BCD and GGL become slower than PGD, APGD and PQN-LBFGS. This is because BCD and GGL require $O(p^4)$ operations in a cycle for solving p nonnegative quadratic programs, where the computational cost grows quickly with the increase of p . In addition, empirically, optGL usually requires less numbers of cycles than BCD and GGL to reach convergence, while the former costs much more time in each cycle than the latter. APGD can be faster than PGD, but that is not a consistent trend.

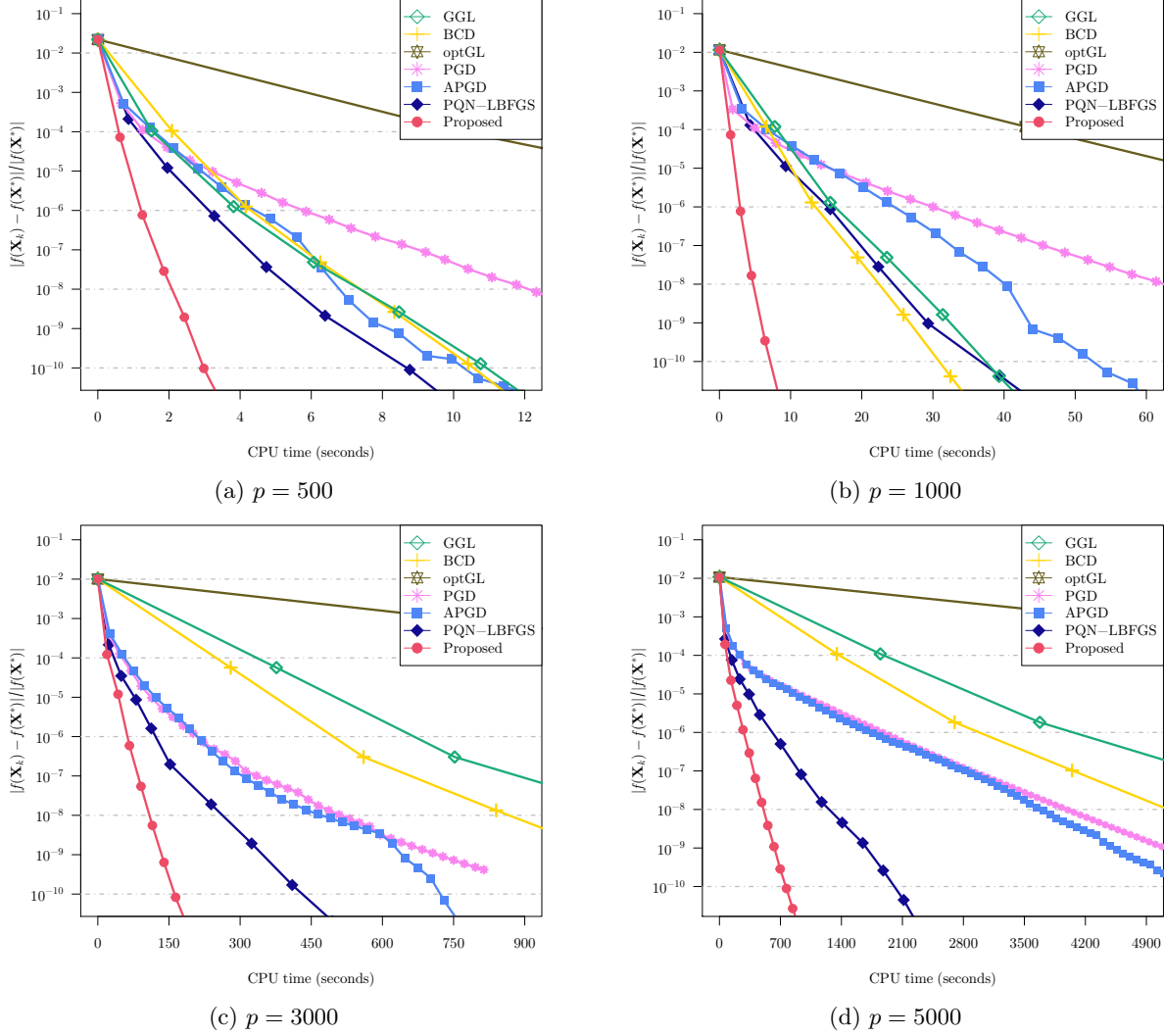
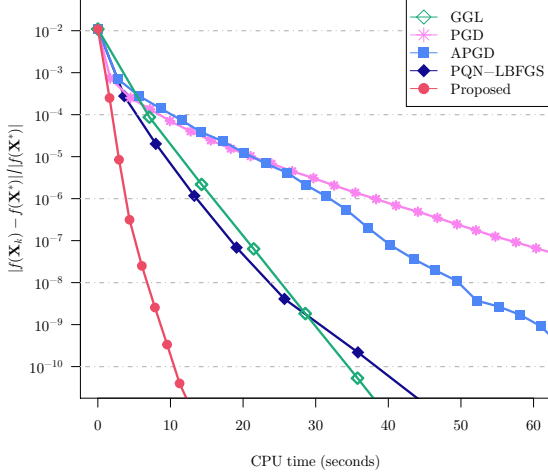
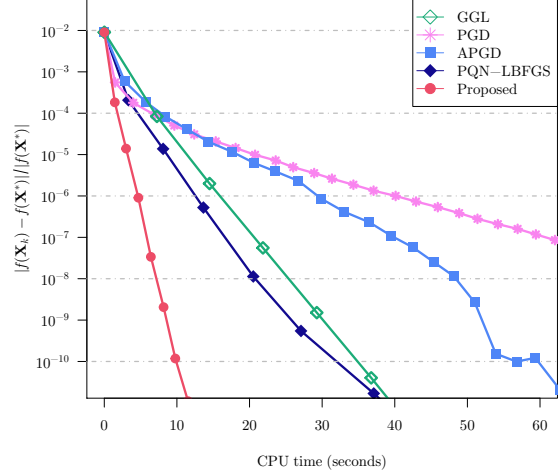


Figure 4: Relative errors of the objective function value versus time on synthetic data sets: BA graphs of degree two consisting of p nodes, (a) $p = 500$, (b) $p = 1000$, (c) $p = 3000$, and (d) $p = 5000$. Note that we plot markers at every 10 iterations for PGD, APGD, PQN-LBFGS, and our proposed FPN, whereas we plot a marker for each cycle of updating all the columns/rows for the BCD-type algorithms BCD, GGL, and optGL. All results are averaged over 10 realizations.

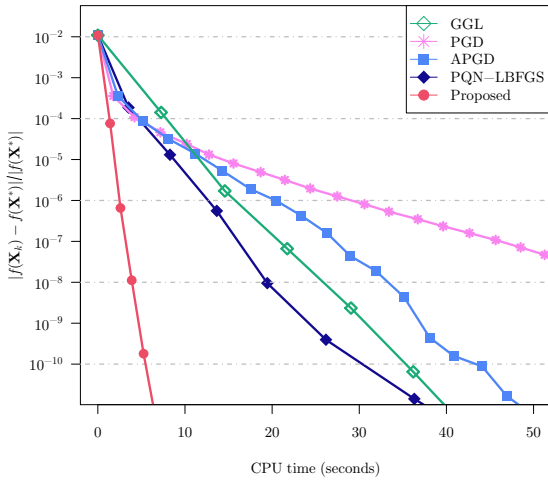
Figure 4 illustrates the computational time of different algorithms in solving Problem (1) on BA graphs of degree two. Similar to the conclusions made on BA graphs of degree one, it is observed that our proposed FPN is always significantly more efficient than the state-of-the-art methods in terms of computational time for different numbers of nodes. Moreover, we observe that PQN-LBFGS and FPN take less iterations to converge to the minimizer than PGD and APGD, especially when the dimension is very high (*e.g.*, $p = 5000$), implying that the former converge faster than the latter. This is because both PQN-LBFGS and FPN exploit the second-order information and use the approximate Newton direction as the search direction, which is useful to overcome the issue of low convergence rate arising from first-order methods in high-dimensional cases. We plot markers at every 10 iterations for PGD, APGD, PQN-LBFGS, and our proposed FPN, whereas we plot a marker for each cycle of updating all columns/rows for the BCD-type algorithms BCD, GGL, and optGL.



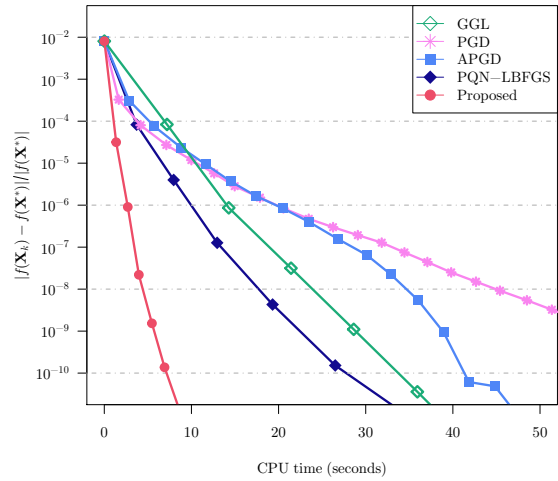
(a) BA graph of degree one imposing 1% disconnectivities



(b) BA graph of degree one imposing 10% disconnectivities



(c) BA graph of degree two imposing 1% disconnectivities



(d) BA graph of degree two imposing 10% disconnectivities

Figure 5: Relative errors of the objective function values versus time in solving Problem (1) on data sets: BA graphs of degree one imposing (a) 1% disconnectivities, (b) 10% disconnectivities, and BA graphs of degree two imposing (c) 1% disconnectivities, (d) 10% disconnectivities. We impose a disconnectivity set \mathcal{E} in Problem (1), which is constructed by randomly collecting 1% or 10% of the indexes corresponding to the zero elements of the underlying precision matrix Θ . Both the two BA graphs consist of 1000 nodes. All results are averaged over 10 realizations.

Figure 5 compares the computational time of different algorithms in solving Problem (1) for the case that a disconnectivity set is imposed. We observe that the proposed FPN always costs the least time to converge to the minimizer. We do not compare with BCD and optGL, because they cannot handle the disconnectivity constraint. PQN-LBFGS originally does not aim to solve the problem with the disconnectivity constraint, thus we update the projection and the construction of the set of *fixed* variables based on our proposed method such that it can handle the disconnectivity constraint. The objective function values of APGD are not guaranteed to be monotonically decreasing during iterations because of the extrapolation step.

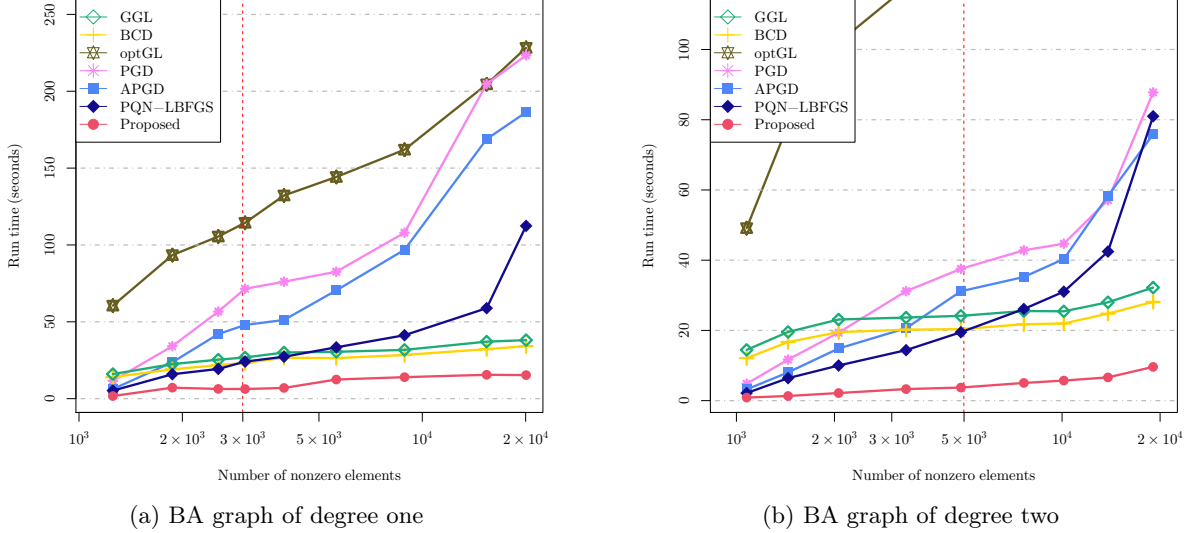


Figure 6: Run time versus numbers of nonzero elements of the estimated precision matrices under different values of the regularization parameter on (a) BA graph of degree one and (b) BA graph of degree two, both consisting of 1000 nodes, where the underlying precision matrices have 2998 and 4994 nonzero elements (indicated by the vertical red lines), respectively. Each algorithm terminates when it achieves $|f(\mathbf{X}_k) - f(\mathbf{X}^*)|/|f(\mathbf{X}^*)| < 10^{-7}$.

Figure 6 evaluates the impact of different values of the regularization parameter σ in (35) on the run time for each algorithm. We observe that the run time of BCD, GGL and FPN remain stable for different values of σ , while the run time of other methods grows as σ decreases. Thus, BCD, GGL and FPN are more robust against the setting of the regularization parameter in terms of the run time. In our experiments, σ takes a sequence of values from 0.02 to 0.0015 to adjust the sparsity level, and all results are averaged over 10 realizations.

5.1.3 Support recovery consistency

In this subsection, we present empirical evidence that the minimizer of Problem (1) recovers the support of the underlying precision matrix correctly given enough samples and the required sample size has approximate logarithmic dependence on the number of nodes.

The required sample size in Theorem 4.6 is $n \geq cd^2 \log(p)$, where p is the number of nodes and d is the maximum number of nonzero elements in each row or column of Θ . To show that n has approximate logarithmic dependence on p , we conduct experiments on ring and grid graphs, where d is always equal to 3 and 5, respectively, independent of p . To make c approximately constant across a range of different numbers of nodes, we generate constant graph weights and collect them into the weighted adjacency matrix \mathbf{A} . Then we generate the underlying precision matrix Θ by the same procedures as adopted in (36).

It is observed in Figure 7 that the probability of successful support recovery for each curve transitions from zero to one as the sample size increases, which is consistent with our theoretical results in Theorem 4.6 that the minimizer of Problem (1) enjoys the support recovery consistency without requiring the *incoherence* condition. We note that all the generated underlying precision matrices Θ do not satisfy the *incoherence* condition in (32). We also observe that the curves corresponding to different numbers of nodes all stack up, implying that the ratio $n/\log p$ acts as an effective sample size in controlling the success of support recovery. Therefore, the sample size n required for successful support recovery has approximate logarithmic dependence on p when c remains approximately constant.

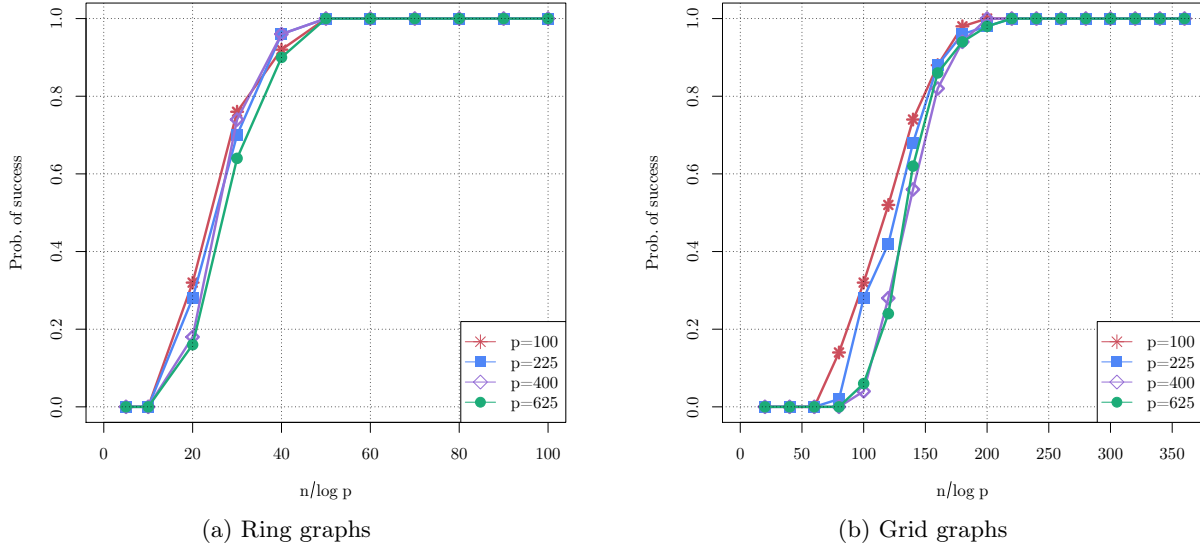


Figure 7: Probability of successful support recovery as a function of the sample size ratio $n/\log p$ on (a) ring graphs, and (b) grid graphs. All results are averaged over 50 realizations.

5.2 Real-world data

In this subsection, we conduct experiments on two real-world data sets: *concepts* data set and financial time-series data set. On the *concepts* data set, we compare the computational time of different algorithms to solve Problem (1). On the financial time-series data set, we present the performance of the minimizer of Problem (1) on the graph edge recovery.

5.2.1 Concepts Data

The *concepts* data set (Lake and Tenenbaum, 2010), collected by Intel Labs, includes 1000 nodes and 218 semantic features, *i.e.*, $p = 1000$ and $n = 218$. Each node denotes a concept such as “house”, “coat”, and “whale”, and each semantic feature is a question such as “Can it fly?”, “Is it alive?”, and “Can you use it?”. The answers are on a five-point scale from “definitely no” to “definitely yes”, conducted on Amazon Mechanical Turk.

Figure 8 illustrates the computational time of different algorithms in solving Problem (1) on the *concepts* data set. We observe that our proposed FPN requires significantly less time to converge to the minimizer than the state-of-the-art algorithms, which is consistent with the observations in synthetic experiments. Note that all the compared algorithms can converge to the minimizer of Problem (1), and thus obtain the same results as shown in Figure 9.

Figure 9 presents a connected subgraph illustrated by the minimizer of Problem (1). Interestingly, it is observed that the learned graph builds a semantic network, where the nodes with related concepts are more closely connected. For example, the concepts related to insects like “bee”, “butterfly”, “flea”, “mosquito”, and “spider” are grouped together, while the concepts related to human such as “baby”, “husband”, “child”, “girls”, and “man” form another group. Moreover, the network shown in Figure 9 connects “penguin” closely to birds like “owl” and “crow”, as well as sea animals like “goldfish” and “seal”, reflecting it as an aquatic bird. To conclude, the learned network can characterize the relationships between concepts well.

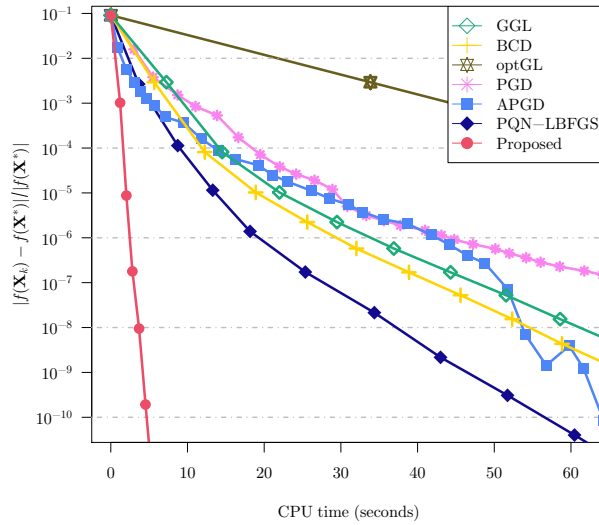


Figure 8: Relative errors of the objective function values versus time for different algorithms in solving Problem (1) on the *concepts* data set, which consists of 1000 nodes.

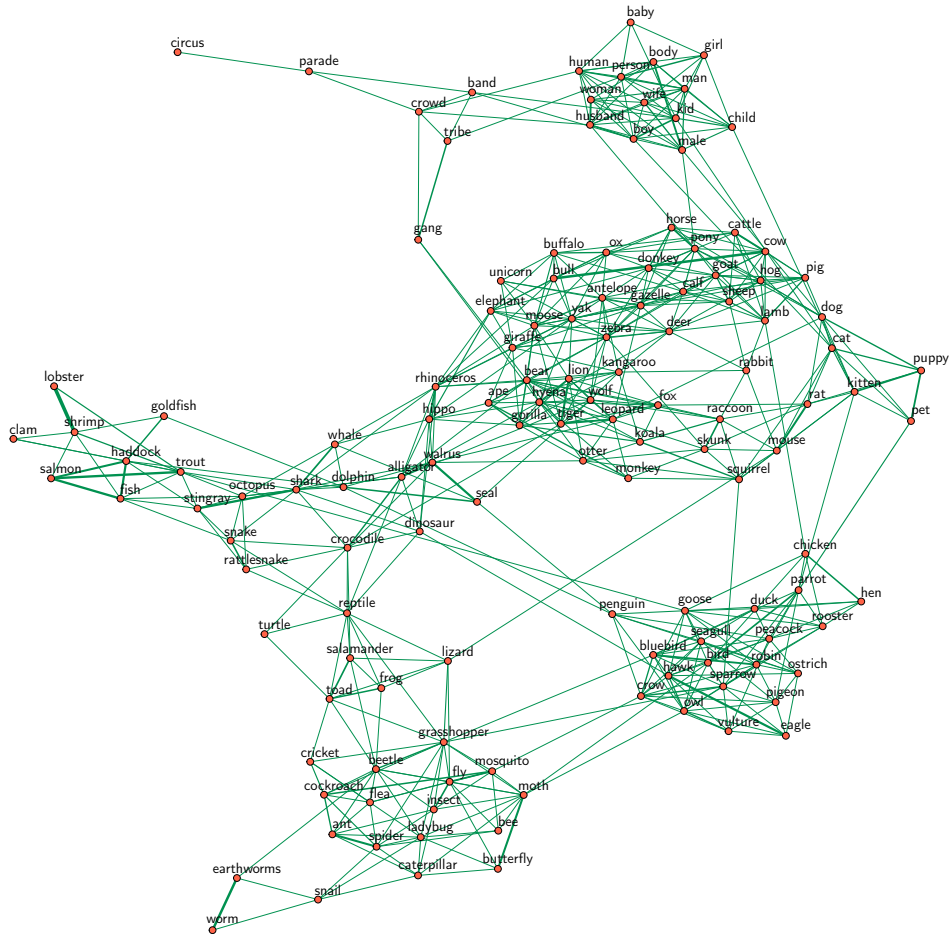


Figure 9: The connected subgraph illustrated by the minimizer \mathbf{X}^* of Problem (1) on the *concepts* data set, which consists of 132 nodes.

5.2.2 Financial Time-series Data

We conduct numerical experiments on the financial time-series data set to verify the performance of the minimizer of Problem (1) on the edge recovery. The MTP₂ models are justified well on stock data since the market factor leads to positive dependencies among stocks (Agrawal et al., 2020). The data is collected from 201 stocks composing the S&P 500 index during the period from Jan. 1st 2017 to Jan. 1st 2020, resulting in 753 observations per stock, *i.e.*, $p = 201$ and $n = 753$. We construct the log-returns data matrix by

$$X_{i,j} = \log P_{i,j} - \log P_{i-1,j},$$

where $P_{i,j}$ denotes the closing price of the j -th stock on the i -th day. The stocks are categorized into 5 sectors by the global industry classification standard (GICS) system (Standard & Poor’s, 2006): Consumer Staples, Utilities, Industrials, Information Technology, and Energy.

Unlike synthetic data, we cannot assess whether the learned graph edges are correct in the financial time-series data since the underlying graph structure is unknown. But we should expect stocks belonging to the same sector to be somewhat linked together. Therefore, we use the *modularity* (Newman, 2006) to measure the performance of edge recovery. Given a graph $\mathcal{G} = (V, E)$, where V is the vertex set and E is the edge set, the *modularity* of the graph is defined by

$$Q := \frac{1}{2|E|} \sum_{i,j \in V} \left(A_{ij} - \frac{d_i d_j}{2|E|} \right) \delta(c_i, c_j), \tag{37}$$

where \mathbf{A} is the adjacency matrix, *i.e.*, $A_{ij} = 1$ if $(i, j) \in E$, and 0 otherwise. The d_i denotes the number of edges connected to node i , c_i denotes the type of node i , and $\delta(\cdot, \cdot)$ is the Kronecker delta function with $\delta(a, b) = 1$ if $a = b$ and 0 otherwise. A stock graph with a high *modularity* value has dense connections between the stocks within the same sector, and has sparse connections between stocks in distinct sectors. A higher *modularity* value indicates a better representation of the actual network of stocks.

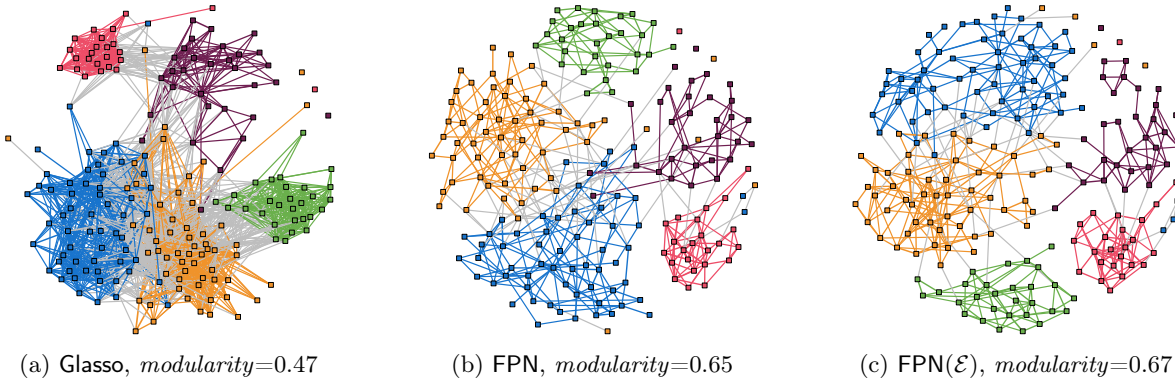


Figure 10: Stock graphs learned via (a) Glasso, (b) FPN, and (c) FPN(\mathcal{E}).

It is observed in Figure 10 that the performances of FPN and FPN(\mathcal{E}) are better than Glasso, since most connections in the graphs learned via FPN and FPN(\mathcal{E}) are between nodes within the same sector, while only few connections (gray-colored edges) exist between nodes from distinct sectors. The *modularity* values for Glasso, FPN, and FPN(\mathcal{E}) are 0.47, 0.65 and 0.67, respectively, implying that FPN and FPN(\mathcal{E}) have a higher degree of interpretability than Glasso. We note that FPN(\mathcal{E}) refers to using FPN to solve Problem (1) imposing a disconnectivity set \mathcal{E} , which is constructed by conducting hard-thresholding on the maximum likelihood estimator that is also used in computing the regularization weights in (35). We also observe that FPN(\mathcal{E}) improves the performance of FPN in a moderate way. We fine-tune the sparsity regularization parameter for each method based on the *modularity* value while allowing only a few isolated nodes. Note that if we further increase the regularization parameter for Glasso, there will exist many isolated nodes which cannot be grouped.

6 Conclusions

In this paper, we have proposed a fast projected Newton-like method to solve the weighted ℓ_1 -norm regularized Gaussian maximum likelihood estimation under MTP_2 constraints. Our proposed algorithm only requires the same orders of computation and memory costs as those of the projected gradient method. The theoretical convergence analysis and the support recovery consistency have been established. Extensive experiments have demonstrated that our algorithm is significantly more efficient than the state-of-the-art methods in terms of computational time. We have applied our method in financial time-series data, and observed a significant performance in terms of *modularity* value on the learned financial networks.

Acknowledgments

We would like to thank Eduardo Pavez for providing the optGL code, and thank Brenden M. Lake for providing the concepts data set.

A Proofs

This section includes the proofs of Proposition 4.1, Theorems 4.3 and 4.6, Corollary 4.4, and Lemmas 3.2 and 3.3.

A.1 Proof of Proposition 4.1

The proof of the existence of the minimizers relies on Lemma A.1 which shows that the lower level set of the objective function of Problem (1) is compact.

We first define the feasible set of Problem (1) as

$$\mathcal{U}^p := \{\mathbf{X} \in \mathbb{R}^{p \times p} \mid \mathbf{X} \in \mathcal{M}^p, X_{ij} = 0, \forall (i, j) \in \mathcal{E}\}. \quad (38)$$

It is clear that the set \mathcal{U}^p is convex. For any $\mathbf{X}_0 \in \mathcal{U}^p$, we define the lower level set of the objective f of Problem (1) as

$$L_f := \{\mathbf{X} \in \mathcal{U}^p \mid f(\mathbf{X}) \leq f(\mathbf{X}_0)\}. \quad (39)$$

Lemma A.1. *Under the same assumption of Proposition 4.1, the lower level set L_f defined in (39) is nonempty and compact, and for any $\mathbf{X} \in L_f$, we have*

$$m\mathbf{I} \preceq \mathbf{X} \preceq M\mathbf{I},$$

for some positive constants m and M .

Proof. We first show that the largest eigenvalue of any $\mathbf{X} \in L_f$ can be upper bounded by M . The objective function of (1) can be written as

$$f(\mathbf{X}) = -\log \det(\mathbf{X}) + \text{tr}(\mathbf{X}\mathbf{G}),$$

where $\mathbf{G} = \mathbf{S} - \boldsymbol{\lambda}$ with $\boldsymbol{\lambda}$ defined in (45). Define two constants as follows

$$\mu := \min_i G_{ii}, \quad \text{and} \quad v := \max_{i \neq j, (i,j) \notin \mathcal{E}} |G_{ij}|.$$

We note that $\mu > 0$ according to the assumption of Lemma A.1. Then one has

$$\text{tr}(\mathbf{X}\mathbf{G}) = \sum_i G_{ii}X_{ii} + \sum_{i \neq j} G_{ij}X_{ij} \geq \mu \text{tr}(\mathbf{X}) + v \sum_{i \neq j} X_{ij}, \quad (40)$$

where the inequality follows from the fact that $X_{ij} \leq 0$ for $i \neq j$, and $X_{ij} = 0$ for $(i, j) \in \mathcal{E}$. We denote the largest eigenvalue of \mathbf{X} by $\lambda_{\max}(\mathbf{X})$. Then we have

$$\lambda_{\max}(\mathbf{X}) \leq \text{tr}(\mathbf{X}) \leq \frac{1}{\mu} \left(\text{tr}(\mathbf{X}\mathbf{G}) + v \sum_{i \neq j} |X_{ij}| \right), \quad (41)$$

where the second inequality follows from (40). In what follows, we bound the terms $\text{tr}(\mathbf{X}\mathbf{G})$ and $\sum_{i \neq j} X_{ij}$. For any $\mathbf{X} \in L_f$, one has

$$f(\mathbf{X}_0) \geq -\log \det(\mathbf{X}) + \text{tr}(\mathbf{X}\mathbf{G}).$$

Therefore, the term $\text{tr}(\mathbf{X}\mathbf{G})$ can be bounded by

$$\text{tr}(\mathbf{X}\mathbf{G}) \leq f(\mathbf{X}_0) + \log \det(\mathbf{X}) \leq f(\mathbf{X}_0) + p \log(\lambda_{\max}(\mathbf{X})). \quad (42)$$

Then one has

$$\sum_{i \neq j} |X_{ij}| \leq \frac{1}{\min_{i \neq j, (i,j) \notin \mathcal{E}} \lambda_{ij}} \sum_{i \neq j} \lambda_{ij} |X_{ij}| \leq \frac{1}{\min_{i \neq j, (i,j) \notin \mathcal{E}} \lambda_{ij}} (f(\mathbf{X}_0) + p \log(\lambda_{\max}(\mathbf{X}))), \quad (43)$$

where the last inequality follows from $\sum_{i \neq j} \lambda_{ij} |X_{ij}| \leq \text{tr}(\mathbf{X}\mathbf{G})$, because $\text{tr}(\mathbf{X}\mathbf{S}) \geq 0$ holds for any $\mathbf{X} \in L_f$ since $\mathbf{X} \in \mathbb{S}_{++}^p$ and $\mathbf{S} \in \mathbb{S}_+^p$. Together with (41), (42) and (43), we obtain

$$\lambda_{\max}(\mathbf{X}) \leq \frac{1}{\mu} \left(1 + \frac{v}{\min_{i \neq j, (i,j) \notin \mathcal{E}} \lambda_{ij}} \right) (f(\mathbf{X}_0) + p \log(\lambda_{\max}(\mathbf{X}))).$$

Considering that $\log(\lambda_{\max}(\mathbf{X}))$ grows much slower than $\lambda_{\max}(\mathbf{X})$, we can conclude that $\lambda_{\max}(\mathbf{X})$ can be upper bounded by a constant M , which depends on $f(\mathbf{X}_0)$, \mathbf{S} , and $\boldsymbol{\lambda}$.

We denote the smallest eigenvalue of \mathbf{X} by $\lambda_{\min}(\mathbf{X})$. For any $\mathbf{X} \in L_f$, one has

$$f(\mathbf{X}_0) \geq f(\mathbf{X}) \geq -\log \det(\mathbf{X}) \geq -\log \lambda_{\min}(\mathbf{X}) - (p-1) \log M.$$

As a result, we have

$$\lambda_{\min}(\mathbf{X}) \geq e^{-f(\mathbf{X}_0)} M^{-(p-1)},$$

which shows that $\lambda_{\min}(\mathbf{X})$ can be lower bounded by a positive constant $m = e^{-f(\mathbf{X}_0)} M^{-(p-1)}$. Finally, we show that the lower level set L_f is compact. First, L_f is closed because f is a continuous function. Second, L_f is also bounded because it is a subset of $\{\mathbf{X} \in \mathbb{R}^{p \times p} | m\mathbf{I} \preceq \mathbf{X} \preceq M\mathbf{I}\}$. \square

Proof of Proposition 4.1. We first prove that Problem (1) has at least one minimizer. It is known by the Weierstrass' extreme value theorem (Drábek and Milota, 2007) that the set of minima is nonempty for any lower semicontinuous function with a nonempty compact lower level set. Therefore, the existence of the minimizers for Problem (1) can be guaranteed by Lemma A.1.

On the other hand, we show that Problem (1) has at most one minimizer by its strict convexity. We have $\nabla^2 f(\mathbf{X}) = \mathbf{X}^{-1} \otimes \mathbf{X}^{-1}$. Thus $\nabla^2 f(\mathbf{X}) \succ \mathbf{0}$ for any \mathbf{X} in the feasible region of Problem (1) defined in (38). Therefore, Problem (1) is strictly convex, and thus has at most one minimizer. Together with the existence of the minimizers, we conclude that Problem (1) has a unique minimizer.

The Lagrangian of the optimization (1) is

$$\mathcal{L}(\mathbf{X}, \mathbf{Y}) = -\log \det(\mathbf{X}) + \text{tr}(\mathbf{X}\mathbf{S}) - \sum_{i \neq j} \lambda_{ij} X_{ij} + \langle \mathbf{Y}, \mathbf{X} \rangle, \quad (44)$$

where \mathbf{Y} is a KKT multiplier with $Y_{ii} = 0$ for $i \in [p]$. We define $\boldsymbol{\lambda}$ by

$$[\boldsymbol{\lambda}]_{ij} = \begin{cases} \lambda_{ij} & \text{if } i \neq j, \\ 0 & \text{otherwise.} \end{cases} \quad (45)$$

It is known that for a convex optimization problem with Slater's condition holding, a pair is primal and dual optimal if and only if the KKT conditions hold. Therefore, the pair $(\mathbf{X}^*, \mathbf{Y}^*)$ is primal and dual optimal if and only if it satisfies the KKT conditions of (1) as below

$$-(\mathbf{X}^*)^{-1} + \mathbf{S} - \boldsymbol{\lambda} + \mathbf{Y}^* = \mathbf{0}; \quad (46)$$

$$X_{ij}^* = 0, \quad \forall (i, j) \in \mathcal{E}; \quad (47)$$

$$X_{ij}^* Y_{ij}^* = 0, \quad X_{ij}^* \leq 0, \quad Y_{ij}^* \geq 0, \quad \forall i \neq j \text{ and } (i, j) \notin \mathcal{E}; \quad (48)$$

$$Y_{ii}^* = 0, \quad \forall i \in [p]. \quad (49)$$

We first prove that the minimizer \mathbf{X}^* must satisfy all the conditions in (23). Note that the KKT conditions (46)-(49) must hold for the minimizer \mathbf{X}^* . Let $\mathcal{V} = \{(i, j) \in [p]^2 \mid X_{ij}^* = 0\}$. First, we have $X_{ij}^* = 0$ for any $(i, j) \in \mathcal{E}$ following from (47). Second, for any (i, j) with $i \neq j$ and $(i, j) \in \mathcal{V}^c$, we have $X_{ij}^* \neq 0$ and $(i, j) \notin \mathcal{E}$. Following from (48), we further obtain $Y_{ij}^* = 0$. Together with (49), we can conclude that $Y_{ij}^* = 0$ for any $(i, j) \in \mathcal{V}^c$. Following from (46), we obtain

$$[\nabla f(\mathbf{X}^*)]_{\mathcal{V}^c} = \mathbf{0}.$$

Note that $(i, i) \in \mathcal{V}^c$ for any $i \in [p]$, because \mathbf{X}^* is positive definite. Then, for any $(i, j) \in \mathcal{V} \setminus \mathcal{E}$, we have $i \neq j$, and thus obtain $Y_{ij}^* \geq 0$ according to (48). Following from (46), we get

$$[\nabla f(\mathbf{X}^*)]_{\mathcal{V} \setminus \mathcal{E}} \leq \mathbf{0}.$$

Now we prove that any point $\mathbf{X}^* \in \mathcal{M}^p$ satisfying the conditions in (23) must be the minimizer, i.e., the KKT conditions (46)-(49) hold for \mathbf{X}^* . We construct \mathbf{Y}^* by $\mathbf{Y}^* = -\nabla f(\mathbf{X}^*)$. First, it is straightforward to check that the conditions (46) and (47) hold. Second, we have

$$[\mathbf{Y}^*]_{\mathcal{V}^c} = -[\nabla f(\mathbf{X}^*)]_{\mathcal{V}^c} = \mathbf{0}. \quad (50)$$

We know that $(i, i) \in \mathcal{V}^c$ for any $i \in [p]$, since $\mathbf{X}^* \in \mathcal{M}^p$. Together with (50), we obtain that the condition (49) holds. Finally, following from the fact that $(i, i) \in \mathcal{V}^c$ for any $i \in [p]$ and $\mathcal{E} \subseteq \mathcal{V}$, we separate the set $\{(i, j) \in [p]^2 \mid i \neq j, (i, j) \notin \mathcal{E}\}$ into two subsets,

$$\{(i, j) \in [p]^2 \mid i \neq j, (i, j) \notin \mathcal{E}\} = \mathcal{I}_1 \cup \mathcal{I}_2,$$

where $\mathcal{I}_1 = \{(i, j) \in [p]^2 \mid (i, j) \in \mathcal{V}^c, i \neq j\}$, and $\mathcal{I}_2 = \{(i, j) \in [p]^2 \mid (i, j) \in \mathcal{V}, (i, j) \notin \mathcal{E}\}$. For any $(i, j) \in \mathcal{I}_1$, we have $Y_{ij}^* = 0$ according to (50), and $X_{ij}^* < 0$ since $\mathbf{X}^* \in \mathcal{M}^p$. Thus the condition (48) holds for any $(i, j) \in \mathcal{I}_1$. For any $(i, j) \in \mathcal{I}_2$, we have $X_{ij}^* = 0$, and $Y_{ij}^* = -[\nabla f(\mathbf{X}^*)]_{ij} \geq 0$ according to the second condition in (23). Thus the condition (48) also holds for any $(i, j) \in \mathcal{I}_2$. Totally, the condition (48) holds. To sum up, all the KKT conditions (46)-(49) hold for any $\mathbf{X}^* \in \mathcal{M}^p$ satisfying the conditions in (23), and thus we can conclude that \mathbf{X}^* is the minimizer of Problem (1). \square

A.2 Proof of Theorem 4.3

Proof. Recall that \mathcal{I}_k^c is the complement of the set \mathcal{I}_k defined in (13). The set \mathcal{I}_k^c can be represented as

$$\mathcal{I}_k^c = \mathcal{T}^c(\mathbf{X}_k, \epsilon_k) \cap \mathcal{E}^c = \bigcup_{l=1}^5 \mathcal{B}_k^{(l)},$$

where $\mathcal{B}_k^{(l)}$, $l = 1, \dots, 5$, are defined as

$$\mathcal{B}_k^{(1)} = \left\{ (i, j) \in \mathcal{E}^c \mid -\epsilon_k \leq [\mathbf{X}_k]_{ij} \leq 0, [\nabla f(\mathbf{X}_k)]_{ij} \geq 0, [\mathbf{P}_k]_{ij} < 0 \right\}, \quad (51)$$

$$\mathcal{B}_k^{(2)} = \left\{ (i, j) \in \mathcal{E}^c \mid -\epsilon_k \leq [\mathbf{X}_k]_{ij} \leq 0, [\nabla f(\mathbf{X}_k)]_{ij} \geq 0, [\mathbf{P}_k]_{ij} \geq 0 \right\}, \quad (52)$$

$$\mathcal{B}_k^{(3)} = \left\{ (i, j) \in \mathcal{E}^c \mid [\mathbf{X}_k]_{ij} < -\epsilon_k, [\mathbf{P}_k]_{ij} < 0 \right\}, \quad (53)$$

$$\mathcal{B}_k^{(4)} = \left\{ (i, j) \in \mathcal{E}^c \mid [\mathbf{X}_k]_{ij} < -\epsilon_k, [\mathbf{P}_k]_{ij} \geq 0 \right\}, \quad (54)$$

$$\mathcal{B}_k^{(5)} = \left\{ (i, j) \in \mathcal{E}^c \mid [\mathbf{X}_k]_{ij} > 0 \right\}, \quad (55)$$

where \mathbf{P}_k is the approximate Newton direction. Each subset $\mathcal{B}_k^{(l)}$ is disjoint with each other. Note that $\mathcal{B}_k^{(5)}$ contains only the indexes corresponding to the diagonal elements of \mathbf{X}_k due to the fact that $\mathbf{X}_k \in \mathcal{M}^p$, while the other subsets include the indexes corresponding to the off-diagonal elements. Then one has, for any $(i, j) \in \mathcal{B}_k^{(1)}$ and $\gamma_k > 0$,

$$0 \leq [\mathbf{X}_{k+1}]_{ij} - [\mathbf{X}_k]_{ij} = [\mathcal{P}_\Omega(\mathbf{X}_k - \gamma \mathbf{P}_k)]_{ij} - [\mathbf{X}_k]_{ij} \leq -\gamma_k [\mathbf{P}_k]_{ij}. \quad (56)$$

For any $(i, j) \in \mathcal{B}_k^{(2)}$ and $\gamma_k > 0$,

$$[\mathbf{X}_{k+1}]_{ij} - [\mathbf{X}_k]_{ij} = [\mathcal{P}_\Omega(\mathbf{X}_k - \gamma \mathbf{P}_k)]_{ij} - [\mathbf{X}_k]_{ij} = -\gamma_k [\mathbf{P}_k]_{ij}.$$

For any $(i, j) \in \mathcal{B}_k^{(3)}$, if the step size satisfies

$$0 < \gamma_k \leq \min_{(i, j) \in \mathcal{B}_k^{(3)}} \frac{\epsilon_k}{|[\mathbf{P}_k]_{ij}|}, \quad (57)$$

then one has

$$[\mathbf{X}_{k+1}]_{ij} - [\mathbf{X}_k]_{ij} = -\gamma_k [\mathbf{P}_k]_{ij}.$$

Similarly, for any $(i, j) \in \mathcal{B}_k^{(4)}$ and $\gamma_k > 0$,

$$[\mathbf{X}_{k+1}]_{ij} - [\mathbf{X}_k]_{ij} = -\gamma_k [\mathbf{P}_k]_{ij}.$$

Finally, for any $(i, j) \in \mathcal{B}_k^{(5)}$, $[\mathbf{X}_k]_{ij}$ must be on the diagonal of \mathbf{X}_k . Therefore, we can directly remove the projection \mathcal{P}_Ω , and obtain

$$[\mathbf{X}_{k+1}]_{ij} - [\mathbf{X}_k]_{ij} = -\gamma_k [\mathbf{P}_k]_{ij}.$$

Therefore, if (57) holds, one has

$$\begin{aligned} & \left\langle \nabla f(\mathbf{X}_k), \mathbf{X}_{k+1} - \mathbf{X}_k \right\rangle \\ &= \sum_{(i, j) \in \mathcal{I}_k^c} [\nabla f(\mathbf{X}_k)]_{ij} \left([\mathbf{X}_{k+1}]_{ij} - [\mathbf{X}_k]_{ij} \right) + \left\langle [\nabla f(\mathbf{X}_k)]_{\mathcal{I}_k}, [\mathbf{X}_{k+1}]_{\mathcal{I}_k} - [\mathbf{X}_k]_{\mathcal{I}_k} \right\rangle \\ &\leq -\gamma_k \left\langle [\nabla f(\mathbf{X}_k)]_{\mathcal{I}_k^c}, [\mathbf{P}_k]_{\mathcal{I}_k^c} \right\rangle + \left\langle [\nabla f(\mathbf{X}_k)]_{\mathcal{I}_k}, [\mathbf{X}_{k+1}]_{\mathcal{I}_k} - [\mathbf{X}_k]_{\mathcal{I}_k} \right\rangle, \end{aligned} \quad (58)$$

where the inequality follows from (51) and (56). One also has

$$\begin{aligned} & \|\mathbf{X}_{k+1} - \mathbf{X}_k\|_{\mathbb{F}}^2 \\ &= \sum_{(i, j) \in \mathcal{I}_k^c} \left([\mathbf{X}_{k+1}]_{ij} - [\mathbf{X}_k]_{ij} \right)^2 + \sum_{(i, j) \in \mathcal{I}_k} \left([\mathbf{X}_{k+1}]_{ij} - [\mathbf{X}_k]_{ij} \right)^2 \\ &\leq \gamma_k^2 \left\langle [\mathbf{P}_k]_{\mathcal{I}_k^c}, [\mathbf{P}_k]_{\mathcal{I}_k^c} \right\rangle - \gamma_k \left\langle [\tilde{\mathbf{D}}_k \odot \nabla f(\mathbf{X}_k)]_{\mathcal{I}_k}, [\mathbf{X}_{k+1}]_{\mathcal{I}_k} - [\mathbf{X}_k]_{\mathcal{I}_k} \right\rangle \\ &\leq \gamma_k^2 \left\langle [\mathbf{P}_k]_{\mathcal{I}_k^c}, [\mathbf{P}_k]_{\mathcal{I}_k^c} \right\rangle - \frac{\epsilon_k}{\|[\nabla f(\mathbf{X}_k)]_{\mathcal{I}_k \setminus \mathcal{E}}\|_{\min}} \left\langle [\nabla f(\mathbf{X}_k)]_{\mathcal{I}_k}, [\mathbf{X}_{k+1}]_{\mathcal{I}_k} - [\mathbf{X}_k]_{\mathcal{I}_k} \right\rangle, \end{aligned} \quad (59)$$

where the first inequality follows from (56) and the iterate of $[\mathbf{X}_{k+1}]_{\mathcal{I}_k}$ in (18), and the second inequality follows from the fact that $[\tilde{\mathbf{D}}_k]_{ij} = \frac{\epsilon_k}{\gamma_k \|\nabla f(\mathbf{X}_k)\|_{ij}}$ for $(i, j) \in \mathcal{T}_k \setminus \mathcal{E}$, in which \mathcal{T}_k denotes $\mathcal{T}(\mathbf{X}_k, \epsilon_k)$. Note that $\mathcal{I}_k = \mathcal{T}_k \cup \mathcal{E}$, and $[\mathbf{X}_k]_{ij} = [\mathbf{X}_{k+1}]_{ij} = 0$ for any $(i, j) \in \mathcal{E}$. Moreover, one has

$$\begin{aligned} \left\langle [\mathbf{P}_k]_{\mathcal{I}_k^c}, [\mathbf{P}_k]_{\mathcal{I}_k^c} \right\rangle &= \left\| [\mathbf{M}_k^{-1}]_{\mathcal{I}_k^c \mathcal{I}_k^c} [\nabla f(\mathbf{X}_k)]_{\mathcal{I}_k^c} \right\|^2 \\ &\leq \left\| [\mathbf{M}_k^{-1}]_{\mathcal{I}_k^c \mathcal{I}_k^c}^{\frac{1}{2}} \right\|_2^2 \left\| [\mathbf{M}_k^{-1}]_{\mathcal{I}_k^c \mathcal{I}_k^c}^{\frac{1}{2}} [\nabla f(\mathbf{X}_k)]_{\mathcal{I}_k^c} \right\|^2 \\ &= \lambda_{\max} \left([\mathbf{M}_k^{-1}]_{\mathcal{I}_k^c \mathcal{I}_k^c} \right) \left\langle [\nabla f(\mathbf{X}_k)]_{\mathcal{I}_k^c}, [\mathbf{P}_k]_{\mathcal{I}_k^c} \right\rangle. \end{aligned} \quad (60)$$

The largest eigenvalue of $[\mathbf{M}_k^{-1}]_{\mathcal{I}_k^c \mathcal{I}_k^c}$ can be bounded by

$$\lambda_{\max} \left([\mathbf{M}_k^{-1}]_{\mathcal{I}_k^c \mathcal{I}_k^c} \right) = \lambda_{\max} \left([\mathbf{H}_k^{-1}]_{\mathcal{I}_k^c \mathcal{I}_k^c} \right) \leq \lambda_{\max} (\mathbf{H}_k^{-1}) = \lambda_{\max} (\mathbf{X}_k \otimes \mathbf{X}_k) \leq M^2, \quad (61)$$

where the first inequality follows from the Eigenvalue Interlacing Theorem, and the second inequality follows from Lemma A.1. Combining (59), (60) and (61), we have

$$\begin{aligned} \|\mathbf{X}_{k+1} - \mathbf{X}_k\|_{\mathbb{F}}^2 &\leq \gamma_k^2 M^2 \left\langle [\nabla f(\mathbf{X}_k)]_{\mathcal{I}_k^c}, [\mathbf{P}_k]_{\mathcal{I}_k^c} \right\rangle \\ &\quad - \frac{\epsilon_k}{\|[\nabla f(\mathbf{X}_k)]_{\mathcal{T}_k \setminus \mathcal{E}}\|_{\min}} \left\langle [\nabla f(\mathbf{X}_k)]_{\mathcal{I}_k}, [\mathbf{X}_{k+1}]_{\mathcal{I}_k} - [\mathbf{X}_k]_{\mathcal{I}_k} \right\rangle. \end{aligned} \quad (62)$$

For any γ_k satisfies

$$0 < \gamma_k \leq \min \left(\frac{2m^2(1-\alpha)}{M^2}, \min_{(i,j) \in \mathcal{B}_k^{(3)}} \frac{\epsilon_k}{|[\mathbf{P}_k]_{ij}|} \right), \quad (63)$$

we can obtain

$$\begin{aligned} &f(\mathbf{X}_{k+1}) - f(\mathbf{X}_k) \\ &\leq \langle \nabla f(\mathbf{X}_k), \mathbf{X}_{k+1} - \mathbf{X}_k \rangle + \frac{1}{2m^2} \|\mathbf{X}_{k+1} - \mathbf{X}_k\|_{\mathbb{F}}^2 \\ &\leq \left(\frac{\gamma_k^2 M^2}{2m^2} - \gamma_k \right) \left\langle [\nabla f(\mathbf{X}_k)]_{\mathcal{I}_k^c}, [\mathbf{P}_k]_{\mathcal{I}_k^c} \right\rangle \\ &\quad + \left(1 - \frac{\epsilon_k}{2m^2 \|[\nabla f(\mathbf{X}_k)]_{\mathcal{T}_\delta \setminus \mathcal{E}}\|_{\min}} \right) \left\langle [\nabla f(\mathbf{X}_k)]_{\mathcal{I}_k}, [\mathbf{X}_{k+1}]_{\mathcal{I}_k} - [\mathbf{X}_k]_{\mathcal{I}_k} \right\rangle \\ &\leq -\alpha \gamma_k \left\langle [\nabla f(\mathbf{X}_k)]_{\mathcal{I}_k^c}, [\mathbf{P}_k]_{\mathcal{I}_k^c} \right\rangle - \alpha \left\langle [\nabla f(\mathbf{X}_k)]_{\mathcal{I}_k}, [\mathbf{X}_k]_{\mathcal{I}_k} - [\mathbf{X}_{k+1}]_{\mathcal{I}_k} \right\rangle, \end{aligned} \quad (64)$$

where the first inequality follows from the results below

$$\lambda_{\max} (\nabla^2 f(\mathbf{X})) = \lambda_{\max} (\mathbf{X}^{-1} \otimes \mathbf{X}^{-1}) = \lambda_{\max}^2 (\mathbf{X}^{-1}) \leq \frac{1}{m^2}, \quad \forall \mathbf{X} \in L_f,$$

where the last inequality follows from Lemma A.1. The second inequality of (64) follows from (58) and (62), and the fact that $\|[\nabla f(\mathbf{X}_k)]_{\mathcal{T}_\delta \setminus \mathcal{E}}\|_{\min} \leq \|[\nabla f(\mathbf{X}_k)]_{\mathcal{T}_k \setminus \mathcal{E}}\|_{\min}$, because $\mathcal{T}_k \subseteq \mathcal{T}_\delta$. The last inequality of (64) follows from (63) and the definition of ϵ_k in (14), and the fact that $\left\langle [\nabla f(\mathbf{X}_k)]_{\mathcal{I}_k^c}, [\mathbf{P}_k]_{\mathcal{I}_k^c} \right\rangle \geq 0$, because $[\mathbf{M}_k^{-1}]_{\mathcal{I}_k^c \mathcal{I}_k^c}$ is positive definite and

$$\left\langle [\nabla f(\mathbf{X}_k)]_{\mathcal{I}_k^c}, [\mathbf{P}_k]_{\mathcal{I}_k^c} \right\rangle = \left\langle [\nabla f(\mathbf{X}_k)]_{\mathcal{I}_k^c}, [\mathbf{M}_k^{-1}]_{\mathcal{I}_k^c \mathcal{I}_k^c} [\nabla f(\mathbf{X}_k)]_{\mathcal{I}_k^c} \right\rangle. \quad (65)$$

Let $\gamma' = \min\left(\frac{2m^2(1-\alpha)}{M^2}, \min_{(i,j) \in \mathcal{B}_k^{(3)}} \frac{\epsilon_k}{\|[\mathbf{P}_k]_{ij}\|}\right)$. Note that γ' is bounded away from zero, because each $[\mathbf{P}_k]_{ij}$ is bounded following from Lemma A.1. We take $\gamma_k = \beta^{m_k}$ with $m_k \leq \min\{m \in \mathbb{N} \mid \beta^m \leq \gamma'\}$, and $\beta^{m_k-1} > \gamma'$. Then we have $\gamma_k > \beta\gamma'$. Therefore, according to (64), we can conclude that for each iteration there must exist a nonzero step size γ_k satisfying (63) such that the Armijo-like step size selection condition holds. We note that the sequence $\{f(\mathbf{X}_k)\}$ is monotonically decreasing before converging, because

$$\begin{aligned} f(\mathbf{X}_{k+1}) - f(\mathbf{X}_k) &\leq -\alpha\gamma_k \left\langle [\nabla f(\mathbf{X}_k)]_{\mathcal{I}_k^c}, [\mathbf{P}_k]_{\mathcal{I}_k^c} \right\rangle - \alpha \left\langle [\nabla f(\mathbf{X}_k)]_{\mathcal{I}_k}, [\mathbf{X}_k]_{\mathcal{I}_k} - [\mathbf{X}_{k+1}]_{\mathcal{I}_k} \right\rangle \\ &\leq -\alpha\gamma_k \left\langle [\nabla f(\mathbf{X}_k)]_{\mathcal{I}_k^c}, [\mathbf{M}_k^{-1}]_{\mathcal{I}_k^c \mathcal{I}_k^c} [\nabla f(\mathbf{X}_k)]_{\mathcal{I}_k^c} \right\rangle \\ &< 0, \end{aligned} \tag{66}$$

where the first inequality follows from the Armijo-like step size selection condition, the second inequality follows from the definition of \mathcal{I}_k in (13), and the last inequality follows from the fact that $[\mathbf{M}_k^{-1}]_{\mathcal{I}_k^c \mathcal{I}_k^c}$ is positive definite.

Following from the facts that the sequence $\{f(\mathbf{X}_k)\}$ is monotonically decreasing and the lower level set is compact according to Lemma A.1, we obtain that the sequence $\{\mathbf{X}_k\}$ is bounded, and thus has at least one limit point. For every limit \mathbf{X}^* of the sequence $\{\mathbf{X}_k\}$, we have $\mathbf{X}^* \in \mathcal{M}^p$, because $\mathbf{X}_k \in \mathcal{M}^p$ can be guaranteed in each iteration. Define

$$\mathcal{I}^* = \mathcal{T}(\mathbf{X}^*, \epsilon^*) \cup \mathcal{E},$$

where $\mathcal{T}(\mathbf{X}^*, \epsilon^*)$ is equal to

$$\mathcal{T}(\mathbf{X}^*, \epsilon^*) = \left\{ (i, j) \in [p]^2 \mid -\epsilon^* \leq [\mathbf{X}^*]_{ij} \leq 0, [\nabla f(\mathbf{X}^*)]_{ij} < 0 \right\},$$

and ϵ^* is defined as

$$\epsilon^* := \min\left(2(1-\alpha)m^2 \|\nabla f(\mathbf{X}^*)\|_{\mathcal{T}_\delta^* \setminus \mathcal{E}} \|\cdot\|_{\min}, \delta\right),$$

where \mathcal{T}_δ^* denotes $\mathcal{T}(\mathbf{X}^*, \delta)$. We note that the Armijo-like step size selection condition allows $\{f(\mathbf{X}_k)\}$ to keep decreasing until $[\mathbf{X}_k]_{\mathcal{I}_k} = \mathbf{0}$, and $[\nabla f(\mathbf{X}_k)]_{\mathcal{I}_k^c} = \mathbf{0}$. Therefore, every limit point \mathbf{X}^* must satisfy

$$[\mathbf{X}^*]_{\mathcal{I}^*} = \mathbf{0}, \quad \text{and} \quad [\nabla f(\mathbf{X}^*)]_{\{\mathcal{I}^*\}^c} = \mathbf{0}. \tag{67}$$

We show that every limit point \mathbf{X}^* is the minimizer of Problem (1) according to Proposition 4.1. Let $\mathcal{V} = \left\{ (i, j) \in [p]^2 \mid [\mathbf{X}^*]_{ij} = 0 \right\}$. First, we have

$$[\mathbf{X}^*]_{ij} = 0, \quad \forall (i, j) \in \mathcal{E},$$

because of the projection \mathcal{P}_Ω in each iteration. Note that $[\mathbf{X}^*]_{ij} = 0$ for any $(i, j) \in \mathcal{I}^*$ according to (67). For any $(i, j) \in \mathcal{V}^c$, i.e., $[\mathbf{X}^*]_{ij} \neq 0$, we must have $(i, j) \in \{\mathcal{I}^*\}^c$. Together with (67),

$$[\nabla f(\mathbf{X}^*)]_{\mathcal{V}^c} = \mathbf{0}$$

holds. For any $(i, j) \in \mathcal{V} \setminus \mathcal{E}$, we must have $(i, j) \in \mathcal{T}(\mathbf{X}^*, \epsilon^*) \cup \{\mathcal{I}^*\}^c$. Recall that $[\nabla f(\mathbf{X}^*)]_{ij} < 0$ for any $(i, j) \in \mathcal{T}(\mathbf{X}^*, \epsilon^*)$, and $[\nabla f(\mathbf{X}^*)]_{ij} = 0$ for any $(i, j) \in \{\mathcal{I}^*\}^c$. Overall, we obtain

$$[\nabla f(\mathbf{X}^*)]_{\mathcal{V} \setminus \mathcal{E}} \leq \mathbf{0}.$$

To sum up, all the conditions in Proposition 4.1 hold for every limit point \mathbf{X}^* , and thus every limit point is the minimizer of Problem (1). Following from the fact that the minimizer of Problem (1) is unique, we

obtain that the limit point of the sequence $\{\mathbf{X}_k\}$ is also unique, and thus $\{\mathbf{X}_k\}$ is convergent. Therefore, we conclude that the sequence $\{\mathbf{X}_k\}$ converges to the unique minimizer of Problem (1).

Finally, we prove that the support of \mathbf{X}^* is consistent with the *free* set \mathcal{I}_k^c for a sufficiently large k . Without loss of generality, we can specify the positive constant δ in (14) as

$$\delta = \omega \min_{(i,j) \in \text{supp}(\mathbf{X}^*)} \left| [\mathbf{X}^*]_{ij} \right|, \quad (68)$$

where $\omega \in (0, 1)$ is a constant.

Note that the sequence $\{\mathbf{X}_k\}$ converges to \mathbf{X}^* . Under Assumption 4.2 that $[\nabla f(\mathbf{X}^*)]_{ij}$ is strictly negative for any $(i, j) \in \text{supp}^c(\mathbf{X}^*) \setminus \mathcal{E}$, there must exist some $a > 0$ and $K_1 \in \mathbb{N}_+$ such that

$$[\nabla f(\mathbf{X}_k)]_{ij} < -\frac{a}{2(1-\alpha)m^2}, \quad \forall (i, j) \in \text{supp}^c(\mathbf{X}^*) \setminus \mathcal{E} \quad (69)$$

holds for any $k \geq K_1$, where $\alpha \in (0, 1)$ is a constant, and m is a positive constant defined in Lemma A.1. We consider a neighbourhood of \mathbf{X}^* defined by

$$\mathcal{N}(\mathbf{X}^*; r) := \{ \mathbf{X} \in \mathbb{R}^{p \times p} \mid \|\mathbf{X} - \mathbf{X}^*\|_F \leq r \}, \quad (70)$$

where r is a positive constant defined as

$$r := \min \left(c \min_{(i,j) \in \text{supp}(\mathbf{X}^*)} \left| [\mathbf{X}^*]_{ij} \right|, a, \delta \right), \quad (71)$$

where $c < 1 - \omega$ is a positive constant. There must exist $K_2 \in \mathbb{N}_+$ such that

$$\mathbf{X}_k \in \mathcal{N}(\mathbf{X}^*; r) \quad (72)$$

holds for any $k \geq K_2$. Moreover,

Take $K_o = \max(K_1, K_2)$. For any $k \geq K_o$ and $(i, j) \in \text{supp}(\mathbf{X}^*)$, one has

$$\left| [\mathbf{X}^*]_{ij} \right| - \left| [\mathbf{X}_k]_{ij} \right| \leq \left| [\mathbf{X}^*]_{ij} - [\mathbf{X}_k]_{ij} \right| \leq \|\mathbf{X}_k - \mathbf{X}^*\|_F \leq r,$$

Thus one can obtain, for any $k \geq K_o$,

$$\left| [\mathbf{X}_k]_{ij} \right| \geq \min_{(i,j) \in \text{supp}(\mathbf{X}^*)} \left| [\mathbf{X}^*]_{ij} \right| - r > \delta > 0, \quad \forall (i, j) \in \text{supp}(\mathbf{X}^*), \quad (73)$$

where the last inequality follows from (68) and (71). Recall that for any $(i, j) \in \mathcal{T}(\mathbf{X}_k, \delta)$,

$$\left| [\mathbf{X}_k]_{ij} \right| \leq \delta. \quad (74)$$

Together with (73) and (74), one has

$$\mathcal{T}(\mathbf{X}_k, \delta) \subseteq \text{supp}^c(\mathbf{X}^*). \quad (75)$$

Then the ϵ_k in (14) can be bounded by

$$\epsilon_k \geq \min \left(2(1-\alpha)m^2 \left\| [\nabla f(\mathbf{X}_k)]_{\text{supp}^c(\mathbf{X}^*) \setminus \mathcal{E}} \right\|_{\min}, \delta \right) \geq \min(a, \delta), \quad (76)$$

where the first inequality follows from (75), and the second inequality follows from (69).

For any $k \geq K_o$ and $(i, j) \in \mathcal{T}(\mathbf{X}_k, \epsilon_k) \cup \mathcal{E}$, one also has

$$\left| [\mathbf{X}_k]_{ij} \right| \leq \epsilon_k \leq \delta. \quad (77)$$

Thus we can obtain

$$\mathcal{T}(\mathbf{X}_k, \epsilon_k) \cup \mathcal{E} \subseteq \text{supp}^c(\mathbf{X}^*). \quad (78)$$

On the other hand, for any $k \geq K_o$ and $(i, j) \in \text{supp}^c(\mathbf{X}^*)$, one has

$$\left| [\mathbf{X}_k]_{ij} \right| = \left| [\mathbf{X}_k]_{ij} - [\mathbf{X}^*]_{ij} \right| \leq \|\mathbf{X}_k - \mathbf{X}^*\|_F \leq r \leq \epsilon_k, \quad (79)$$

where the last inequality follows from (71) and (76). Therefore, one has

$$\text{supp}^c(\mathbf{X}^*) \subseteq \mathcal{T}(\mathbf{X}_k, \epsilon_k) \cup \mathcal{E} \cup \mathcal{B}_k^{(1)} \cup \mathcal{B}_k^{(2)},$$

where $\mathcal{B}_k^{(1)}$ and $\mathcal{B}_k^{(2)}$ are defined in (51) and (52), respectively. Note that $\mathcal{B}_k^{(5)} \cap \text{supp}^c(\mathbf{X}^*) = \emptyset$, because any $(i, j) \in \mathcal{B}_k^{(5)}$ corresponds to an element $[\mathbf{X}^*]_{ij}$ on the diagonal which must be nonzero. Moreover, following from (69), one has

$$(\text{supp}^c(\mathbf{X}^*) \setminus \mathcal{E}) \cap \mathcal{B}_k^{(1)} = \emptyset, \quad \text{and} \quad (\text{supp}^c(\mathbf{X}^*) \setminus \mathcal{E}) \cap \mathcal{B}_k^{(2)} = \emptyset.$$

Therefore, we can obtain

$$\text{supp}^c(\mathbf{X}^*) \subseteq \mathcal{T}(\mathbf{X}_k, \epsilon_k) \cup \mathcal{E}. \quad (80)$$

Combining (78) and (80) yields

$$\text{supp}^c(\mathbf{X}^*) = \mathcal{T}(\mathbf{X}_k, \epsilon_k) \cup \mathcal{E} = \mathcal{I}_k. \quad (81)$$

Equivalently, we have

$$\text{supp}(\mathbf{X}^*) = \mathcal{I}_k^c, \quad \forall k \geq K_o. \quad (82)$$

We can see that the sets of *restricted* and *free* variables, \mathcal{I}_k and \mathcal{I}_k^c , are fixed for any $k \geq K_o$. Therefore, for any $k \geq K_o$,

$$[\mathbf{X}_{k+1}]_{\mathcal{I}_{k+1}} = [\mathbf{X}_{k+1}]_{\mathcal{I}_k} = \mathbf{0}, \quad (83)$$

where the second equality follows from the iterate of \mathbf{X}_{k+1} . Moreover, together with (73) and (82), we obtain that for any $k \geq K_o$,

$$[\mathbf{X}_{k+1}]_{\mathcal{I}_{k+1}^c} \neq \mathbf{0}. \quad (84)$$

Take $k_o = K_o + 1$. Combining (83) and (84) yields

$$\text{supp}(\mathbf{X}_k) = \mathcal{I}_k^c, \quad \forall k \geq k_o. \quad (85)$$

Therefore, together with (82) and (85), we conclude that

$$\text{supp}(\mathbf{X}^*) = \text{supp}(\mathbf{X}_k) = \mathcal{I}_k^c, \quad \forall k \geq k_o. \quad (86)$$

□

A.3 Proof of Corollary 4.4

Proof. Corollary 4.4 is a direct extension of the result in Bertsekas (2016). Let g be twice continuously differentiable and consider the following iterate

$$\mathbf{x}_{x+1} = \mathbf{x}_k - \gamma_k \mathbf{D}_k \nabla g(\mathbf{x}_k),$$

where \mathbf{D}_k is positive definite and symmetric. Then the sequence $\{\mathbf{x}_k\}$ admits the following convergence result (Bertsekas, 2016),

$$\limsup_{k \rightarrow \infty} \frac{\|\mathbf{x}_{k+1} - \mathbf{x}^*\|_{\mathbf{D}_k^{-1}}^2}{\|\mathbf{x}_k - \mathbf{x}^*\|_{\mathbf{D}_k^{-1}}^2} = \limsup_{k \rightarrow \infty} \max \left(|1 - \gamma_k m'_k|^2, |1 - \gamma_k M'_k|^2 \right), \quad (87)$$

where \mathbf{x}^* is the limit of the sequence $\{\mathbf{x}_k\}$, which satisfies that $\nabla g(\mathbf{x}^*) = \mathbf{0}$ and $\nabla^2 g(\mathbf{x}^*)$ is positive definite, and m'_k and M'_k are the smallest and largest eigenvalues of $(\mathbf{D}_k)^{1/2} \nabla^2 g(\mathbf{x}_k) (\mathbf{D}_k)^{1/2}$, respectively. This conclusion is extended from the convergence result for the quadratic objective function. Conceptually, this makes sense because a twice continuously differentiable objective function is very close to a positive definite quadratic function in the neighborhood of a non-singular local minimum.

Note that we have established in (86) that for any $k \geq k_o$,

$$\text{supp}(\mathbf{X}_k) = \text{supp}(\mathbf{X}^*).$$

Therefore, the support of \mathbf{X}_k is fixed and consistent with that of the minimizer for any $k \geq k_o$. As a result, we can remove the projection \mathcal{P}_Ω , and use the iterate \mathbf{X}_{k+1} as follows,

$$[\mathbf{X}_{k+1}]_{\mathcal{I}_k} = \mathbf{0}, \quad \text{and} \quad [\mathbf{X}_{k+1}]_{\mathcal{I}_k^c} = [\mathbf{X}_k]_{\mathcal{I}_k^c} - \gamma_k [\mathbf{P}_k]_{\mathcal{I}_k^c}.$$

Then for any $k \geq k_o$, we can rewrite the iterate $[\mathbf{X}_{k+1}]_{\mathcal{I}_k^c}$ as

$$[\mathbf{X}_{k+1}]_{\mathcal{I}_k^c} = [\mathbf{X}_k]_{\mathcal{I}_k^c} - \gamma_k \mathbf{R}_k^{-1} [\nabla f(\mathbf{X}_k)]_{\mathcal{I}_k^c}, \quad (88)$$

where $\mathbf{R}_k^{-1} = [\mathbf{H}_k^{-1}]_{\mathcal{I}_k^c \mathcal{I}_k^c}$. We can see that the iterate (88) reduces to an iterate of an unconstrained optimization algorithm on the subspace. Now, we can follow from the results in (87) and obtain

$$\limsup_{k \rightarrow \infty} \frac{\|[\mathbf{X}_{k+1}]_{\mathcal{I}_k^c} - [\mathbf{X}^*]_{\mathcal{I}_k^c}\|_{\mathbf{R}_k}^2}{\|[\mathbf{X}_k]_{\mathcal{I}_k^c} - [\mathbf{X}^*]_{\mathcal{I}_k^c}\|_{\mathbf{R}_k}^2} = \limsup_{k \rightarrow \infty} \max \left(|1 - \gamma_k m_k|^2, |1 - \gamma_k M_k|^2 \right), \quad (89)$$

where m_k and M_k are the smallest and largest eigenvalues of $\mathbf{R}_k^{-\frac{1}{2}} [\mathbf{H}_k]_{\mathcal{I}_k^c \mathcal{I}_k^c} \mathbf{R}_k^{-\frac{1}{2}}$, respectively. Following from (17), (86), and the equality that $\mathbf{R}_k^{-1} = [\mathbf{H}_k^{-1}]_{\mathcal{I}_k^c \mathcal{I}_k^c}$, we obtain

$$\|[\mathbf{X}_k]_{\mathcal{I}_k^c} - [\mathbf{X}^*]_{\mathcal{I}_k^c}\|_{\mathbf{R}_k}^2 = \|\mathbf{X}_k - \mathbf{X}^*\|_{\mathbf{M}_k}^2, \quad \forall k \geq k_o. \quad (90)$$

When $k \geq k_o$, the backtracking exit condition reduces to

$$f(\mathbf{X}_{k+1}) \leq f(\mathbf{X}_k) - \alpha \gamma_k \left\langle [\nabla f(\mathbf{X}_k)]_{\mathcal{I}_k^c}, [\mathbf{P}_k]_{\mathcal{I}_k^c} \right\rangle.$$

Similar to the unconstrained case, the step size must satisfy the backtracking exit condition if $\gamma_k \geq \min(1, 2(1 - \alpha)\beta/M_k)$ (Bertsekas, 1976) as $k \rightarrow \infty$. Then together with (89) and (90), we conclude that

$$\limsup_{k \rightarrow \infty} \frac{\|\mathbf{X}_{k+1} - \mathbf{X}^*\|_{\mathbf{M}_k}^2}{\|\mathbf{X}_k - \mathbf{X}^*\|_{\mathbf{M}_k}^2} \leq \limsup_{k \rightarrow \infty} \left(1 - \min \left(m_k, \frac{2(1 - \alpha)\beta m_k}{M_k} \right) \right)^2.$$

□

A.4 Proof of Theorem 4.6

Proof. Recall that the \mathbf{X}^* is the minimizer of Problem (1). We define an oracle estimator $\hat{\mathbf{X}}$ by

$$\begin{aligned} \hat{\mathbf{X}} := & \arg \min_{\mathbf{X} \in \mathcal{M}^p} && -\log \det(\mathbf{X}) + \text{tr}(\mathbf{X}\mathbf{S}) + \sum_{i \neq j} \lambda_{ij} |X_{ij}|, \\ & \text{subject to} && X_{ij} = 0, \quad \forall (i, j) \in \mathcal{S}^c, \end{aligned} \quad (91)$$

where \mathcal{S}^c is the complement of the support set of the underlying precision matrix Θ . Note that the set \mathcal{S}^c only contains the indexes of the off-diagonal elements because of the fact that $\Theta \in \mathcal{M}^p$.

The Lagrangian of the optimization (91) is

$$\hat{L}(\mathbf{X}, \mathbf{Y}) = -\log \det(\mathbf{X}) + \text{tr}(\mathbf{X}\mathbf{S}) - \sum_{i \neq j} \lambda_{ij} X_{ij} + \langle \mathbf{Y}, \mathbf{X} \rangle,$$

where \mathbf{Y} is a KKT multiplier with $Y_{ii} = 0$ for $i \in [p]$. With a similar argument for the KKT system in (46)-(49) for Problem (1), the pair $(\hat{\mathbf{X}}, \hat{\mathbf{Y}})$ is primal and dual optimal if and only if it satisfies the KKT system of (91) as below

$$-\hat{\mathbf{X}}^{-1} + \mathbf{S} - \boldsymbol{\lambda} + \hat{\mathbf{Y}} = \mathbf{0}; \quad (92)$$

$$\hat{X}_{ij} = 0, \quad \forall (i, j) \in \mathcal{S}^c; \quad (93)$$

$$\hat{X}_{ij} \hat{Y}_{ij} = 0, \quad \hat{X}_{ij} \leq 0, \quad \hat{Y}_{ij} \geq 0, \quad \forall (i, j) \in \mathcal{S}_{\text{off}}; \quad (94)$$

$$\hat{Y}_{ii} = 0, \quad \forall i \in [p]; \quad (95)$$

where $\mathcal{S}_{\text{off}} = \{(i, j) \in [p]^2 \mid \Theta_{ij} < 0, i \neq j\}$, i.e., the set of indexes corresponding to the nonzero off-diagonal elements of Θ . Recall that $\mathcal{S}' = \mathcal{S}^c \setminus \mathcal{E}$ and $\mathcal{E} \subseteq \mathcal{S}^c$. Then we can check that, if

$$\hat{Y}_{ij} = [\hat{\mathbf{X}}^{-1}]_{ij} - S_{ij} + \lambda_{ij} \geq 0 \quad (96)$$

holds for any $(i, j) \in \mathcal{S}'$, then $(\hat{\mathbf{X}}, \hat{\mathbf{Y}})$ also satisfies the KKT system of (1) as shown in (46)-(49), implying that $\mathbf{X}^* = \hat{\mathbf{X}}$.

In what follows, we aim to establish (96). Define a function $h : \mathbb{R}^{|\mathcal{S}|} \rightarrow \mathbb{R}^{|\mathcal{S}|}$,

$$h(\boldsymbol{\Delta}_{\mathcal{S}}) = - \left[\left(\Theta + \widetilde{\boldsymbol{\Delta}}_{\mathcal{S}} \right)^{-1} \right]_{\mathcal{S}} + \mathbf{S}_{\mathcal{S}} - \boldsymbol{\lambda}_{\mathcal{S}},$$

where the notation $\mathbf{X}_{\mathcal{S}} \in \mathbb{R}^{|\mathcal{S}|}$ denotes a vector containing all the elements of \mathbf{X} in the set \mathcal{S} , and $\widetilde{\mathbf{X}}_{\mathcal{S}} \in \mathbb{R}^{p \times p}$ denotes a matrix defined by

$$\left[\widetilde{\mathbf{X}}_{\mathcal{S}} \right]_{ij} = \begin{cases} X_{ij} & \text{if } (i, j) \in \mathcal{S}, \\ 0 & \text{otherwise.} \end{cases}$$

Define a function $g : \mathbb{R}^{|\mathcal{S}|} \rightarrow \mathbb{R}^{|\mathcal{S}|}$

$$g(\boldsymbol{\Delta}_{\mathcal{S}}) = -(\mathbf{H}_{\mathcal{S}\mathcal{S}})^{-1} h(\boldsymbol{\Delta}_{\mathcal{S}}) + \boldsymbol{\Delta}_{\mathcal{S}}, \quad (97)$$

where \mathbf{H} is the Hessian matrix at Θ . We consider a region

$$\mathcal{B}(r) := \left\{ \boldsymbol{\Delta}_{\mathcal{S}} \in \mathbb{R}^{|\mathcal{S}|} \mid \|\boldsymbol{\Delta}_{\mathcal{S}}\|_{\max} \leq r, \widetilde{\boldsymbol{\Delta}}_{\mathcal{S}} = \widetilde{\boldsymbol{\Delta}}_{\mathcal{S}}^{\top} \right\}, \quad \text{with } r := \frac{4}{3} K_H \|\boldsymbol{\lambda}_{\mathcal{S}}\|_{\max}. \quad (98)$$

Recall that we specify the regularization parameter $\lambda_{ij} = C_{ij} \sqrt{\frac{\log p}{n}}$, where C_{ij} is a positive constant. Let $c_1 = \max_{(i,j) \in \mathcal{S}} |C_{ij}|$. Then we have $\|\boldsymbol{\lambda}_{\mathcal{S}}\|_{\max} = c_1 \sqrt{\frac{\log p}{n}}$. When the sample size is lower bounded by

$$n \geq cd^2 \log p \quad \text{with } c = \left(4c_1 K_H K_{\Sigma} \max \left(4K_H K_{\Sigma}^2 \max \left(\frac{\|\mathbf{C}_{\mathcal{S}}\|_{\max}}{\|\mathbf{C}_{\mathcal{S}'}\|_{\min}}, 1 \right), 1 \right) \right)^2, \quad (99)$$

we have

$$r \leq \min \left(\frac{1}{3dK_{\Sigma}}, \frac{1}{12dK_H K_{\Sigma}^3} \min \left(1, \frac{\|\mathbf{C}_{\mathcal{S}'}\|_{\min}}{\|\mathbf{C}_{\mathcal{S}}\|_{\max}} \right) \right). \quad (100)$$

For any $\boldsymbol{\Delta}_{\mathcal{S}} \in \mathcal{B}(r)$, we have

$$\left\| \Theta^{-1} \widetilde{\boldsymbol{\Delta}}_{\mathcal{S}} \right\|_{\infty} \leq \left\| \Theta^{-1} \right\|_{\infty} \left\| \widetilde{\boldsymbol{\Delta}}_{\mathcal{S}} \right\|_{\infty} \leq K_{\Sigma} d \|\boldsymbol{\Delta}_{\mathcal{S}}\|_{\max} \leq \frac{1}{3}, \quad (101)$$

where the second inequality follows from the definition of K_Σ in (28) and the fact that Θ has at most d nonzero elements in any row, and the last inequality follows from (100). The (101) can guarantee that $(\Theta + \widetilde{\Delta}_S)^{-1}$ is invertible. We can further obtain the convergent matrix expansion,

$$\begin{aligned}
(\Theta + \widetilde{\Delta}_S)^{-1} &= (I + \Theta^{-1} \widetilde{\Delta}_S)^{-1} \Theta^{-1} \\
&= \sum_{k=0}^{\infty} (-1)^k (\Theta^{-1} \widetilde{\Delta}_S)^k \Theta^{-1} \\
&= \Theta^{-1} - \Theta^{-1} \widetilde{\Delta}_S \Theta^{-1} + \sum_{k=2}^{\infty} (-1)^k (\Theta^{-1} \widetilde{\Delta}_S)^k \Theta^{-1} \\
&= \Theta^{-1} - \Theta^{-1} \widetilde{\Delta}_S \Theta^{-1} + \Theta^{-1} \widetilde{\Delta}_S \Theta^{-1} \widetilde{\Delta}_S N \Theta^{-1},
\end{aligned} \tag{102}$$

where $N = \sum_{k=0}^{\infty} (-1)^k (\Theta^{-1} \widetilde{\Delta}_S)^k$. Define $R(\Delta)$ as

$$R(\Delta) = (\Theta + \Delta)^{-1} - \Theta^{-1} + \Theta^{-1} \Delta \Theta^{-1}. \tag{103}$$

Then we have

$$\begin{aligned}
R(\widetilde{\Delta}_S) &= (\Theta + \widetilde{\Delta}_S)^{-1} - \Theta^{-1} + \Theta^{-1} \widetilde{\Delta}_S \Theta^{-1} \\
&= \Theta^{-1} \widetilde{\Delta}_S \Theta^{-1} \widetilde{\Delta}_S N \Theta^{-1},
\end{aligned}$$

where the second equality follows from (102). We now bound the term $R(\widetilde{\Delta}_S)$ as follows

$$\begin{aligned}
\|R(\widetilde{\Delta}_S)\|_{\max} &= \max_{i,j} |e_i^\top \Theta^{-1} \widetilde{\Delta}_S \Theta^{-1} \widetilde{\Delta}_S N \Theta^{-1} e_j| \\
&\leq \max_i \|e_i^\top \Theta^{-1} \widetilde{\Delta}_S\|_{\max} \max_j \|\Theta^{-1} \widetilde{\Delta}_S N \Theta^{-1} e_j\|_1 \\
&\leq \max_i \|e_i^\top \Theta^{-1}\|_1 \|\widetilde{\Delta}_S\|_{\max} \max_j \|\Theta^{-1} \widetilde{\Delta}_S N \Theta^{-1} e_j\|_1 \\
&= \|\Theta^{-1}\|_{\infty} \|\widetilde{\Delta}_S\|_{\max} \|\Theta^{-1} \widetilde{\Delta}_S N \Theta^{-1}\|_1 \\
&\leq \|\widetilde{\Delta}_S\|_{\max} \|\widetilde{\Delta}_S\|_{\infty} \|N^\top\|_{\infty} \|\Theta^{-1}\|_{\infty}^3 \\
&\leq \frac{3}{2} d K_\Sigma^3 \|\Delta_S\|_{\max}^2,
\end{aligned}$$

where the first inequality follows from the fact that $|a^\top b| \leq \|a\|_{\max} \|b\|_1$ holds for any $a, b \in \mathbb{R}^p$; the second inequality is established by the inequality that $\|a^\top B\|_{\max} \leq \|a\|_1 \|B\|_{\max}$ for any $a \in \mathbb{R}^p$ and $B \in \mathbb{R}^{p \times q}$; the third inequality follows from $\|A\|_1 = \|A^\top\|_{\infty}$ and the sub-multiplicativity of $\|\cdot\|_{\infty}$; the last inequality follows from $\|\|\widetilde{\Delta}_S\|\|_{\infty} \leq d \|\|\widetilde{\Delta}_S\|\|_{\max}$ since there are at most d nonzero elements in each row and column of $\widetilde{\Delta}_S$, and the bound of the term $\|N^\top\|_{\infty}$ in the following

$$\|N^\top\|_{\infty} \leq \sum_{k=0}^{\infty} \|\|\widetilde{\Delta}_S \Theta^{-1}\|\|_{\infty}^k \leq \frac{1}{1 - \|\|\widetilde{\Delta}_S\|\|_{\infty} \|\|\Theta^{-1}\|\|_{\infty}} \leq \frac{3}{2},$$

where the last inequality follows from (101).

For any $\mathbf{\Delta}_S \in \mathbb{B}(r)$ with $r \leq \min\left(\frac{1}{3dK_\Sigma}, \frac{1}{12dK_H K_\Sigma^3} \min\left(1, \frac{\|\mathbf{C}_{S'}\|_{\min}}{\|\mathbf{C}_S\|_{\max}}\right)\right)$, we have

$$\left\| \mathbf{R}\left(\widetilde{\mathbf{\Delta}}_S\right) \right\|_{\max} \leq \frac{r}{8K_H} \min\left(1, \frac{\|\mathbf{C}_{S'}\|_{\min}}{\|\mathbf{C}_S\|_{\max}}\right) = \frac{1}{6} \min\left(\|\boldsymbol{\lambda}_S\|_{\max}, \|\boldsymbol{\lambda}_{S'}\|_{\min}\right), \quad (104)$$

where the equality follows from the definition of r in (98).

We can rewrite the function g in (97) as

$$\begin{aligned} g(\mathbf{\Delta}_S) &= -(\mathbf{H}_{SS})^{-1} \left(- \left[\left(\boldsymbol{\Theta} + \widetilde{\mathbf{\Delta}}_S \right)^{-1} \right]_S + \mathbf{S}_S - \boldsymbol{\lambda}_S \right) + \mathbf{\Delta}_S \\ &= -(\mathbf{H}_{SS})^{-1} \left(- \left[\boldsymbol{\Theta}^{-1} \right]_S + \left[\boldsymbol{\Theta}^{-1} \widetilde{\mathbf{\Delta}}_S \boldsymbol{\Theta}^{-1} \right]_S \right. \\ &\quad \left. - \left[\boldsymbol{\Theta}^{-1} \widetilde{\mathbf{\Delta}}_S \boldsymbol{\Theta}^{-1} \widetilde{\mathbf{\Delta}}_S \mathbf{N} \boldsymbol{\Theta}^{-1} \right]_S + \mathbf{S}_S - \boldsymbol{\lambda}_S \right) + \mathbf{\Delta}_S. \end{aligned}$$

Following from the fact that

$$\text{vec}\left(\boldsymbol{\Theta}^{-1} \mathbf{\Delta} \boldsymbol{\Theta}^{-1}\right) = \left(\boldsymbol{\Theta}^{-1} \otimes \boldsymbol{\Theta}^{-1}\right) \text{vec}(\mathbf{\Delta}) = \mathbf{H} \text{vec}(\mathbf{\Delta}),$$

we can obtain

$$\left[\boldsymbol{\Theta}^{-1} \widetilde{\mathbf{\Delta}}_S \boldsymbol{\Theta}^{-1} \right]_S = \mathbf{H}_{SS} \mathbf{\Delta}_S. \quad (105)$$

Let $\mathbf{G} = \mathbf{S} - \boldsymbol{\Theta}^{-1}$. Following from (105), we obtain

$$g(\mathbf{\Delta}_S) = (\mathbf{H}_{SS})^{-1} \left(\left[\mathbf{R}\left(\widetilde{\mathbf{\Delta}}_S\right) \right]_S - \mathbf{G}_S + \boldsymbol{\lambda}_S \right).$$

For any $\mathbf{\Delta}_S \in \mathcal{B}(r)$, we bound $g(\mathbf{\Delta}_S)$ as follows,

$$\begin{aligned} \|g(\mathbf{\Delta}_S)\|_{\max} &\leq \left\| (\mathbf{H}_{SS})^{-1} \right\|_{\infty} \left(\left\| \left[\mathbf{R}\left(\widetilde{\mathbf{\Delta}}_S\right) \right]_S \right\|_{\max} + \|\mathbf{G}_S\|_{\max} + \|\boldsymbol{\lambda}_S\|_{\max} \right) \\ &\leq K_H \left(\frac{1}{3} \min\left(\|\boldsymbol{\lambda}_S\|_{\max}, \|\boldsymbol{\lambda}_{S'}\|_{\min}\right) + \|\boldsymbol{\lambda}_S\|_{\max} \right) \\ &\leq r, \end{aligned} \quad (106)$$

where the second inequality follows from the condition in (30) that

$$\|\mathbf{G}\|_{\max} \leq \frac{1}{6} \min\left(\|\boldsymbol{\lambda}_S\|_{\max}, \|\boldsymbol{\lambda}_{S'}\|_{\min}\right), \quad (107)$$

and (104), and the last inequality in (106) follows from the definition of r in (98). We also have

$$\left[\mathbf{R}\left(\widetilde{\mathbf{\Delta}}_S\right) \right]_S - \mathbf{G}_S + \boldsymbol{\lambda}_S = \left[\boldsymbol{\Theta}^{-1} g(\widetilde{\mathbf{\Delta}}_S) \boldsymbol{\Theta}^{-1} \right]_S = \left[\boldsymbol{\Theta}^{-1} g(\widetilde{\mathbf{\Delta}}_S)^\top \boldsymbol{\Theta}^{-1} \right]_S,$$

where the last equality follows from the fact that $\mathbf{R}\left(\widetilde{\mathbf{\Delta}}_S\right)$, \mathbf{G} and $\boldsymbol{\lambda}$ are all symmetric. Since $g(\mathbf{\Delta}_S)$ is injective, we can obtain

$$g(\widetilde{\mathbf{\Delta}}_S) = g(\widetilde{\mathbf{\Delta}}_S)^\top.$$

Together with (106), we conclude that $g(\mathbf{\Delta}_S) \in \mathcal{B}(r)$ for any $\mathbf{\Delta}_S \in \mathcal{B}(r)$. Therefore, $g(\mathbf{\Delta}_S)$ is a continuous self mapping in the convex compact set $\mathcal{B}(r)$. Following from the Brouwer fixed-point theorem, we obtain that there exists a fixed point $\widetilde{\mathbf{\Delta}}_S$ such that $g(\widetilde{\mathbf{\Delta}}_S) = \widetilde{\mathbf{\Delta}}_S$, i.e., $h(\widetilde{\mathbf{\Delta}}_S) = \mathbf{0}$. Then we have

$$- \left[\left(\boldsymbol{\Theta} + \widetilde{\mathbf{\Delta}}_S \right)^{-1} \right]_S + \mathbf{S}_S - \boldsymbol{\lambda}_S = \mathbf{0}. \quad (108)$$

We construct $\hat{\mathbf{X}}$ by

$$\hat{\mathbf{X}} = \mathbf{\Theta} + \widetilde{\bar{\Delta}}_{\mathcal{S}},$$

and $\hat{\mathbf{Y}}$ by

$$\hat{Y}_{ij} = \begin{cases} [\hat{\mathbf{X}}^{-1} - \mathbf{S} + \boldsymbol{\lambda}]_{ij} & \text{if } (i, j) \in \mathcal{S}^c, \\ 0 & \text{otherwise.} \end{cases}$$

We can check that this pair $(\hat{\mathbf{X}}, \hat{\mathbf{Y}})$ satisfies the KKT system of Problem (91) as shown in (92)-(95). Note that we have

$$\hat{X}_{ij} < 0, \quad \forall (i, j) \in \mathcal{S}_{\text{off}}, \quad (109)$$

which follows from Assumption 4.5 that $\min_{(i,j) \in \mathcal{S}_{\text{off}}} |\Theta_{ij}| > \frac{4}{3} K_H \|\boldsymbol{\lambda}_{\mathcal{S}}\|_{\max}$.

According to (103), one obtains

$$\mathbf{R}(\widetilde{\bar{\Delta}}_{\mathcal{S}}) = \hat{\mathbf{X}}^{-1} - \mathbf{\Theta}^{-1} + \mathbf{\Theta}^{-1} \widetilde{\bar{\Delta}}_{\mathcal{S}} \mathbf{\Theta}^{-1}.$$

Let $\boldsymbol{\Xi} = \hat{\mathbf{X}}^{-1} - \mathbf{S}$. Then we obtain

$$\mathbf{\Theta}^{-1} \widetilde{\bar{\Delta}}_{\mathcal{S}} \mathbf{\Theta}^{-1} - \mathbf{R}(\widetilde{\bar{\Delta}}_{\mathcal{S}}) + \mathbf{G} + \boldsymbol{\Xi} = \mathbf{0}. \quad (110)$$

We can rewrite (110) by *vectorizing* the matrices, and get

$$\mathbf{H} \text{vec}(\widetilde{\bar{\Delta}}_{\mathcal{S}}) - \text{vec}(\mathbf{R}(\widetilde{\bar{\Delta}}_{\mathcal{S}})) + \text{vec}(\mathbf{G}) + \text{vec}(\boldsymbol{\Xi}) = \mathbf{0}.$$

We decompose the equality into two blocks with respect to \mathcal{S} and \mathcal{S}' and obtain

$$\mathbf{H}_{\mathcal{S}\mathcal{S}} \bar{\Delta}_{\mathcal{S}} - [\mathbf{R}(\widetilde{\bar{\Delta}}_{\mathcal{S}})]_{\mathcal{S}} + \mathbf{G}_{\mathcal{S}} + \boldsymbol{\Xi}_{\mathcal{S}} = \mathbf{0},$$

and

$$\mathbf{H}_{\mathcal{S}'\mathcal{S}} \bar{\Delta}_{\mathcal{S}} - [\mathbf{R}(\widetilde{\bar{\Delta}}_{\mathcal{S}})]_{\mathcal{S}'} + \mathbf{G}_{\mathcal{S}'} + \boldsymbol{\Xi}_{\mathcal{S}'} = \mathbf{0}.$$

By eliminating $\bar{\Delta}_{\mathcal{S}}$, we can get

$$\begin{aligned} \|\boldsymbol{\Xi}_{\mathcal{S}'}\|_{\max} &\leq \left\| \mathbf{H}_{\mathcal{S}'\mathcal{S}} (\mathbf{H}_{\mathcal{S}\mathcal{S}})^{-1} \right\|_{\infty} \left(\|\mathbf{G}_{\mathcal{S}}\|_{\max} + \left\| [\mathbf{R}(\widetilde{\bar{\Delta}}_{\mathcal{S}})]_{\mathcal{S}} \right\|_{\max} \right) \\ &\quad + \left\| \mathbf{H}_{\mathcal{S}'\mathcal{S}} (\mathbf{H}_{\mathcal{S}\mathcal{S}})^{-1} \boldsymbol{\Xi}_{\mathcal{S}} \right\|_{\max} + \left(\|\mathbf{G}_{\mathcal{S}'}\|_{\max} + \left\| [\mathbf{R}(\widetilde{\bar{\Delta}}_{\mathcal{S}})]_{\mathcal{S}'} \right\|_{\max} \right). \end{aligned} \quad (111)$$

According to (108), we have

$$\|\boldsymbol{\Xi}_{\mathcal{S}}\|_{\max} = \|\boldsymbol{\lambda}_{\mathcal{S}}\|_{\max}.$$

Combining (104), (107) and (111) yields

$$\|\boldsymbol{\Xi}_{\mathcal{S}'}\|_{\max} \leq \frac{4}{3} \left\| \mathbf{H}_{\mathcal{S}'\mathcal{S}} (\mathbf{H}_{\mathcal{S}\mathcal{S}})^{-1} \right\|_{\infty} \|\boldsymbol{\lambda}_{\mathcal{S}}\|_{\max} + \frac{1}{3} \|\boldsymbol{\lambda}_{\mathcal{S}'}\|_{\min} \leq \|\boldsymbol{\lambda}_{\mathcal{S}'}\|_{\min}, \quad (112)$$

where the last inequality follows from the condition that

$$\frac{\|\boldsymbol{\lambda}_{\mathcal{S}'}\|_{\min}}{\|\boldsymbol{\lambda}_{\mathcal{S}}\|_{\max}} = \frac{\|\mathbf{C}_{\mathcal{S}'}\|_{\min}}{\|\mathbf{C}_{\mathcal{S}}\|_{\max}} \geq 2 \left\| \mathbf{H}_{\mathcal{S}'\mathcal{S}} (\mathbf{H}_{\mathcal{S}\mathcal{S}})^{-1} \right\|_{\infty}.$$

By establishing (112), we obtain

$$\max_{(i,j) \in \mathcal{S}'} \left| [\hat{\mathbf{X}}^{-1}]_{ij} - S_{ij} \right| \leq \min_{(i,j) \in \mathcal{S}'} \lambda_{ij}.$$

Therefore, we can conclude that (96) holds. As a result, we obtain that $\mathbf{X}^* = \hat{\mathbf{X}}$.

According to the definition of $\hat{\mathbf{X}}$ in (91), we get that for any $(i, j) \in \mathcal{S}^c$, where $\mathcal{S}^c = \{(i, j) \mid \Theta_{ij} = 0\}$, we have $[\hat{\mathbf{X}}]_{ij} = 0$. Meanwhile, following from (109) and the fact that $[\hat{\mathbf{X}}]_{ii} \neq 0$ for any $i \in [p]$, we have $[\hat{\mathbf{X}}]_{ij} \neq 0$ for any $(i, j) \in \mathcal{S}$. Therefore, we can establish that $\text{supp}(\hat{\mathbf{X}}) = \text{supp}(\mathbf{\Theta})$, and thus $\text{supp}(\mathbf{X}^*) = \text{supp}(\mathbf{\Theta})$. \square

A.5 Proof of Lemma 3.2

Proof. The Hessian matrix at \mathbf{X}_k has the form:

$$\mathbf{H}_k = \mathbf{X}_k^{-1} \otimes \mathbf{X}_k^{-1}.$$

Then we obtain

$$\mathbf{H}_k^{-1} = \mathbf{X}_k \otimes \mathbf{X}_k.$$

Following from the property of Kronecker product that $\text{vec}(\mathbf{ABC}) = (\mathbf{C}^\top \otimes \mathbf{A}) \text{vec}(\mathbf{B})$, we obtain

$$\text{vec}(\mathbf{P}_k) = \mathbf{H}_k^{-1} \text{vec}(\nabla f(\mathbf{X}_k)) = \text{vec}(\mathbf{X}_k \nabla f(\mathbf{X}_k) \mathbf{X}_k).$$

Therefore, we have

$$\mathbf{P}_k = \mathbf{X}_k \nabla f(\mathbf{X}_k) \mathbf{X}_k.$$

□

A.6 Proof of Lemma 3.3

Proof. Following from (7), (16) and (17), we obtain

$$[\mathbf{P}_k]_{\mathcal{I}_k^c} = [\mathbf{H}_k^{-1}]_{\mathcal{I}_k^c \mathcal{I}_k^c} [\nabla f(\mathbf{X}_k)]_{\mathcal{I}_k^c} = \left[\mathbf{H}_k^{-1} \text{vec}(\mathcal{P}_{\mathcal{I}_k^c}(\nabla f(\mathbf{X}_k))) \right]_{\mathcal{I}_k^c},$$

where the projection $\mathcal{P}_{\mathcal{I}_k^c}$ is defined in (20). Following from the fact that $\text{vec}(\mathbf{ABC}) = (\mathbf{C}^\top \otimes \mathbf{A}) \text{vec}(\mathbf{B})$ and $\mathbf{H}_k^{-1} = \mathbf{X}_k \otimes \mathbf{X}_k$, we have

$$\mathbf{H}_k^{-1} \text{vec}(\mathcal{P}_{\mathcal{I}_k^c}(\nabla f(\mathbf{X}_k))) = \text{vec}(\mathbf{X}_k \mathcal{P}_{\mathcal{I}_k^c}(\nabla f(\mathbf{X}_k)) \mathbf{X}_k).$$

By collecting the elements in the set \mathcal{I}_k^c , we obtain

$$[\mathbf{P}_k]_{\mathcal{I}_k^c} = [\mathbf{X}_k \mathcal{P}_{\mathcal{I}_k^c}(\nabla f(\mathbf{X}_k)) \mathbf{X}_k]_{\mathcal{I}_k^c}.$$

□

References

- Raj Agrawal, Uma Roy, and Caroline Uhler. Covariance Matrix Estimation under Total Positivity for Portfolio Selection. *Journal of Financial Econometrics*, 09 2020. doi: 10.1093/jjfinec/nbaa018.
- Animashree Anandkumar, Vincent YF Tan, Furong Huang, and Alan S Willsky. High-dimensional Gaussian graphical model selection: Walk summability and local separation criterion. *Journal of Machine Learning Research*, 13(Aug):2293–2337, 2012.
- Onureena Banerjee, Laurent El Ghaoui, and Alexandre d’Aspremont. Model selection through sparse maximum likelihood estimation for multivariate Gaussian or binary data. *Journal of Machine Learning Research*, 9(Mar):485–516, 2008.
- Albert-László Barabási and Réka Albert. Emergence of scaling in random networks. *Science*, 286(5439):509–512, 1999.
- Johnathan M Bardsley and Curtis R Vogel. A nonnegatively constrained convex programming method for image reconstruction. *SIAM Journal on Scientific Computing*, 25(4):1326–1343, 2004.

- Dimitri P Bertsekas. On the Goldstein-Levitin-Polyak gradient projection method. *IEEE Transactions on Automatic Control*, 21(2):174–184, 1976.
- Dimitri P Bertsekas. Projected Newton methods for optimization problems with simple constraints. *SIAM Journal on Control and Optimization*, 20(2):221–246, 1982.
- Dimitri P Bertsekas. *Nonlinear programming*. Athena Scientific, Belmont, MA, third edition, 2016.
- Erik Bølviken. Probability inequalities for the multivariate normal with non-negative partial correlations. *Scandinavian Journal of Statistics*, pages 49–58, 1982.
- Emmanuel J Candes, Michael B Wakin, and Stephen P Boyd. Enhancing sparsity by reweighted ℓ_1 minimization. *Journal of Fourier analysis and applications*, 14(5):877–905, 2008.
- José Vinícius de Miranda Cardoso, Jiaxi Ying, and Daniel Perez Palomar. Algorithms for learning graphs in financial markets. *arXiv preprint arXiv:2012.15410*, 2020.
- Jinghui Chen, Pan Xu, Lingxiao Wang, Jian Ma, and Quanquan Gu. Covariate adjusted precision matrix estimation via nonconvex optimization. In *Proceedings of the 35th International Conference on Machine Learning*, volume 80, pages 921–930, 2018.
- Alexandre d’Aspremont, Onureena Banerjee, and Laurent El Ghaoui. First-order methods for sparse covariance selection. *SIAM Journal on Matrix Analysis and Applications*, 30(1):56–66, 2008.
- Michel Denuit, Jan Dhaene, Marc Goovaerts, and Rob Kaas. *Actuarial theory for dependent risks: measures, orders and models*. John Wiley & Sons, 2006.
- Quoc Tran Dinh, Anastasios Kyriklidis, and Volkan Cevher. A proximal Newton framework for composite minimization: Graph learning without Cholesky decompositions and matrix inversions. In *Proceedings of the 30th International Conference on Machine Learning*, volume 28, pages 271–279, 2013.
- Xiaowen Dong, Dorina Thanou, Michael Rabbat, and Pascal Frossard. Learning graphs from data: A signal representation perspective. *IEEE Signal Processing Magazine*, 36(3):44–63, 2019.
- Pavel Drábek and Jaroslav Milota. *Methods of nonlinear analysis: applications to differential equations*. Springer Science & Business Media, 2007.
- John Duchi, Stephen Gould, and Daphne Koller. Projected subgradient methods for learning sparse Gaussians. In *Proceedings of the Twenty-Fourth Conference on Uncertainty in Artificial Intelligence*, page 153–160, 2008.
- Hilmi E Egilmez, Eduardo Pavez, and Antonio Ortega. Graph learning from data under Laplacian and structural constraints. *IEEE Journal of Selected Topics in Signal Processing*, 11(6):825–841, 2017.
- Shaun Fallat, Steffen Lauritzen, Kayvan Sadeghi, Caroline Uhler, Nanny Wermuth, and Piotr Zwiernik. Total positivity in Markov structures. *The Annals of Statistics*, 45(3):1152–1184, 2017.
- Jerome Friedman, Trevor Hastie, and Robert Tibshirani. Sparse inverse covariance estimation with the graphical lasso. *Biostatistics*, 9(3):432–441, 2008.
- Eli M Gafni and Dimitri P Bertsekas. Two-metric projection methods for constrained optimization. *SIAM Journal on Control and Optimization*, 22(6):936–964, 1984.
- James Lincoln Herring, James Nagy, and Lars Ruthotto. Gauss–Newton optimization for phase recovery from the bispectrum. *IEEE Transactions on Computational Imaging*, 6:235–247, 2019.

- Jean Honorio, Dimitris Samaras, Irina Rish, and Guillermo Cecchi. Variable selection for Gaussian graphical models. In *Proceedings of the Fifteenth International Conference on Artificial Intelligence and Statistics*, volume 22, pages 538–546, 2012.
- Cho Hsieh, Inderjit S Dhillon, Pradeep K Ravikumar, and Mátyás A Sustik. Sparse inverse covariance matrix estimation using quadratic approximation. In *Advances in Neural Information Processing Systems*, volume 24, pages 2330–2338, 2011.
- Cho-Jui Hsieh, Arindam Banerjee, Inderjit S Dhillon, and Pradeep K Ravikumar. A divide-and-conquer method for sparse inverse covariance estimation. In *Advances in Neural Information Processing Systems*, volume 25, pages 2330–2338, 2012.
- Cho-Jui Hsieh, Mátyás A Sustik, Inderjit S Dhillon, Pradeep K Ravikumar, and Russell Poldrack. BIG & QUIC: Sparse inverse covariance estimation for a million variables. In *Advances in Neural Information Processing Systems*, volume 26, pages 3165–3173, 2013.
- Cho-Jui Hsieh, Mátyás A Sustik, Inderjit S Dhillon, and Pradeep Ravikumar. QUIC: quadratic approximation for sparse inverse covariance estimation. *The Journal of Machine Learning Research*, 15(1):2911–2947, 2014.
- Álvaro Barbero Jiménez and Suvrit Sra. Fast Newton-type methods for total variation regularization. In *Proceedings of the 28th International Conference on International Conference on Machine Learning*, pages 313–320, 2011.
- Samuel Karlin and Yosef Rinott. M-matrices as covariance matrices of multinormal distributions. *Linear Algebra and its Applications*, 52:419–438, 1983.
- Jonathan Kelner, Frederic Koehler, Raghu Meka, and Ankur Moitra. Learning some popular Gaussian graphical models without condition number bounds. In *Advances in Neural Information Processing Systems*, volume 33, pages 10986–10998, 2020.
- Dongmin Kim, Suvrit Sra, and Inderjit S Dhillon. Fast Newton-type methods for the least squares nonnegative matrix approximation problem. In *Proceedings of the 2007 SIAM International Conference on Data Mining*, pages 343–354, 2007.
- Dongmin Kim, Suvrit Sra, and Inderjit S Dhillon. Tackling box-constrained optimization via a new projected Quasi-Newton approach. *SIAM Journal on Scientific Computing*, 32(6):3548–3563, 2010.
- Sandeep Kumar, Jiayi Ying, José Vinícius de M Cardoso, and Daniel P Palomar. A unified framework for structured graph learning via spectral constraints. *Journal of Machine Learning Research*, 21(22):1–60, 2020.
- Brenden Lake and Joshua Tenenbaum. Discovering structure by learning sparse graphs. In *Proceedings of the 33rd Annual Cognitive Science Conference*, pages 778–783, 2010.
- Germana Landi and Elena Loli Piccolomini. An improved Newton projection method for nonnegative deblurring of Poisson-corrupted images with Tikhonov regularization. *Numerical Algorithms*, 60(1):169–188, 2012.
- Germana Landi and Elena Loli Piccolomini. Nptool: a Matlab software for nonnegative image restoration with Newton projection methods. *Numerical Algorithms*, 62(3):487–504, 2013.
- Steffen Lauritzen, Caroline Uhler, and Piotr Zwiernik. Maximum likelihood estimation in Gaussian models under total positivity. *The Annals of Statistics*, 47(4):1835–1863, 2019.

- Steffen Lauritzen, Caroline Uhler, and Piotr Zwiernik. Total positivity in exponential families with application to binary variables. *The Annals of Statistics*, 49(3):1436–1459, 2021.
- Lu Li and Kim-Chuan Toh. An inexact interior point method for L_1 -regularized sparse covariance selection. *Mathematical Programming Computation*, 2(3):291–315, 2010.
- Qiang Liu and Alexander Ihler. Learning scale free networks by reweighted ℓ_1 regularization. In *Proceedings of the Fourteenth International Conference on Artificial Intelligence and Statistics*, volume 15, pages 40–48, 2011.
- Zhaosong Lu. Smooth optimization approach for sparse covariance selection. *SIAM Journal on Optimization*, 19(4):1807–1827, 2009.
- Dmitry M Malioutov, Jason K Johnson, and Alan S Willsky. Walk-sums and belief propagation in Gaussian graphical models. *Journal of Machine Learning Research*, 7:2031–2064, 2006.
- Rahul Mazumder and Trevor Hastie. The graphical lasso: New insights and alternatives. *Electronic Journal of Statistics*, 6:2125, 2012.
- Calvin McCarter and Seyoung Kim. Large-scale optimization algorithms for sparse conditional Gaussian graphical models. In *Proceedings of the 19th International Conference on Artificial Intelligence and Statistics*, volume 51, pages 528–537, 2016.
- Nicolai Meinshausen and Peter Bühlmann. High-dimensional graphs and variable selection with the lasso. *The Annals of Statistics*, 34(3):1436–1462, 2006.
- Yurii Nesterov. *Introductory lectures on convex optimization: A basic course*, volume 87. Springer Science & Business Media, 2003.
- Yurii E Nesterov. A method for solving the convex programming problem with convergence rate $O(1/k^2)$. *Proceedings of the USSR Academy of Sciences*, 269:543–547, 1983.
- Mark EJ Newman. Modularity and community structure in networks. *Proceedings of the National Academy of Sciences*, 103(23):8577–8582, 2006.
- Jorge Nocedal. Updating quasi-Newton matrices with limited storage. *Mathematics of Computation*, 35(151):773–782, 1980.
- Jorge Nocedal and Stephen Wright. *Numerical optimization*. Springer Science & Business Media, 2006.
- Antonio Ortega, Pascal Frossard, Jelena Kovačević, José MF Moura, and Pierre Vandergheynst. Graph signal processing: Overview, challenges, and applications. *Proceedings of the IEEE*, 106(5):808–828, 2018.
- Figen Oztoprak, Jorge Nocedal, Steven Rennie, and Peder A Olsen. Newton-like methods for sparse inverse covariance estimation. In *Advances in Neural Information Processing Systems*, volume 25, pages 755–763, 2012.
- Eduardo Pavez and Antonio Ortega. Generalized Laplacian precision matrix estimation for graph signal processing. In *2016 IEEE International Conference on Acoustics, Speech and Signal Processing*, pages 6350–6354, 2016.
- Eduardo Pavez, Hilmi E Egilmez, and Antonio Ortega. Learning graphs with monotone topology properties and multiple connected components. *IEEE Transactions on Signal Processing*, 66(9):2399–2413, 2018.

- Pradeep Ravikumar, Martin J Wainwright, Garvesh Raskutti, and Bin Yu. High-dimensional covariance estimation by minimizing ℓ_1 -penalized log-determinant divergence. *Electronic Journal of Statistics*, 5: 935–980, 2011.
- Dimitri Rothmel and Thomas Schuster. Solving an inverse heat convection problem with an implicit forward operator by using a projected quasi-Newton method. *Inverse Problems*, 37(4):045014, 2021.
- Katya Scheinberg and Irina Rish. Learning sparse Gaussian Markov networks using a greedy coordinate ascent approach. In *Joint European Conference on Machine Learning and Knowledge Discovery in Databases*, pages 196–212, 2010.
- Katya Scheinberg, Shiqian Ma, and Donald Goldfarb. Sparse inverse covariance selection via alternating linearization methods. In *Advances in Neural Information Processing Systems*, volume 23, pages 2101–2109, 2010.
- Mark Schmidt, Ewout Berg, Michael Friedlander, and Kevin Murphy. Optimizing costly functions with simple constraints: A limited-memory projected Quasi-Newton algorithm. In *Proceedings of the Twelfth International Conference on Artificial Intelligence and Statistics*, volume 5, pages 456–463, 2009.
- Gesualdo Scutari, Francisco Facchinei, Peiran Song, Daniel P Palomar, and Jong-Shi Pang. Decomposition by partial linearization: Parallel optimization of multi-agent systems. *IEEE Transactions on Signal Processing*, 62(3):641–656, 2014.
- Ali Shojaie and George Michailidis. Penalized likelihood methods for estimation of sparse high-dimensional directed acyclic graphs. *Biometrika*, 97(3):519–538, 2010.
- David I Shuman, Sunil K Narang, Pascal Frossard, Antonio Ortega, and Pierre Vandergheynst. The emerging field of signal processing on graphs: Extending high-dimensional data analysis to networks and other irregular domains. *IEEE Signal Processing Magazine*, 30(3):83–98, 2013.
- Martin Slawski and Matthias Hein. Estimation of positive definite M-matrices and structure learning for attractive Gaussian Markov random fields. *Linear Algebra and its Applications*, 473:145–179, 2015.
- Jake A Soloff, Adityanand Guntuboyina, and Michael I Jordan. Covariance estimation with nonnegative partial correlations. *arXiv preprint arXiv:2007.15252*, 2020.
- Standard & Poor’s. Global Industry Classification Standard (GICS). *Tech Report*, 2006.
- Joel A Tropp. Just relax: Convex programming methods for identifying sparse signals in noise. *IEEE Transactions on Information Theory*, 52(3):1030–1051, 2006.
- Chengjing Wang, Defeng Sun, and Kim-Chuan Toh. Solving log-determinant optimization problems by a Newton-CG primal proximal point algorithm. *SIAM Journal on Optimization*, 20(6):2994–3013, 2010.
- Yuhao Wang, Uma Roy, and Caroline Uhler. Learning high-dimensional Gaussian graphical models under total positivity without adjustment of tuning parameters. In *Proceedings of the Twenty Third International Conference on Artificial Intelligence and Statistics*, volume 108, pages 2698–2708, 2020.
- Matt Wytock, Suvrit Sra, and J. Zico Kolter. Fast Newton methods for the group fused lasso. In *Proceedings of the Thirtieth Conference on Uncertainty in Artificial Intelligence*, pages 888–897, 2014.
- Yue Xie and Stephen J Wright. Complexity of projected Newton methods for bound-constrained optimization. *arXiv preprint arXiv:2103.15989*, 2021.
- Eunho Yang, Genevera Allen, Zhandong Liu, and Pradeep K Ravikumar. Graphical models via generalized linear models. In *Advances in Neural Information Processing Systems*, volume 25, pages 1358–1366, 2012.

- Eunho Yang, Pradeep Ravikumar, Genevera I Allen, and Zhandong Liu. Graphical models via univariate exponential family distributions. *Journal of Machine Learning Research*, 16(1):3813–3847, 2015.
- Ming Yuan and Yi Lin. Model selection and estimation in the Gaussian graphical model. *Biometrika*, 94(1): 19–35, 2007.
- Peng Zhao and Bin Yu. On model selection consistency of Lasso. *The Journal of Machine Learning Research*, 7:2541–2563, 2006.
- Hui Zou. The adaptive lasso and its oracle properties. *Journal of the American Statistical Association*, 101 (476):1418–1429, 2006.